IEEE Access
Multidisciplinary ⋮ Rapid Review ⋮ Open Access Journal

Received September 13, 2020, accepted September 18, 2020, date of publication September 22, 2020,
date of current version October 5, 2020.

Digital Object Identifier 10.1109/ACCESS.2020.3025907

Application of Computer Simulation Method in Deep Underground Engineering of Complicated Geological Condition

YUE WU[1,2], WEIGUO QIAO[1,2], SHUAI ZHANG[1,2], ZONGHAO ZHANG[3], YANZHI LI[1,2], ZHENWANG FAN[1,2], AND LEI ZHANG[1,2]

[1]Shandong Key Laboratory of Civil Engineering Disaster Prevention and Mitigation, Shandong University of Science and Technology, Qingdao 266590, China
[2]College of Civil Engineering and Architecture, Shandong University of Science and Technology, Qingdao 266590, China
[3]Shandong Iron and Steel Group Real Estate Company, Ltd., Qingdao 266071, China

Corresponding author: Weiguo Qiao (qiaowg1@163.com)

This work was supported in part by the National Natural Science Foundation of China under Grant 51774192 and Grant 51704183.

ABSTRACT Computer simulation technology is used to solve various engineering problems in the new century, particularly exemplified by the widespread use of numerical simulation research methods. Due to the complicated geological environment, a mine tunnel with a depth of 850 m in Hebei Province has caused various problems, such as large displacements and difficulty in implementing support schemes. However, the complex geological conditions make the project unique, and support schemes for other projects cannot be simply copied. In addition, due to engineering cost requirements, repeatedly evaluating different on-site support schemes is unacceptable. Therefore, it is necessary to obtain an appropriate support scheme through computer simulation technology. Consequently, by implementing FLAC^{3D} software and using the progressive design method (PDM), a variety of support schemes are designed, and simulation tests, such as analysis and optimization of parameters, are performed. The research results show that through the analysis of stress, displacement and other aspects of the various schemes designed by using PDM, the finally selected scheme that was applied to the actual project achieved good results. The findings have proven the feasibility of the method, and the method can guide engineering problems under similar geological conditions.

INDEX TERMS Computer numerical simulation, FlAC^{3D}, PDM, practical engineering application, deep coal mine roadway support.

I. INTRODUCTION

With the advancement of science and technology, people can use computers to perform simulation calculations to solve problems in practical engineering and are no longer confined to field attempts. Numerical simulation is a common research method. From a macro perspective, Bingqian *et al.* [1] summarized the research methods and results of numerical simulation of the wind-induced response of power transmission towers from multiple aspects and noted their advantages and disadvantages and future development directions. Relying on numerical simulation software for high-temperature and high-salt oil reservoirs, Rui *et al.* [2] established a mathematical model to better guide actual engineering; and accurately describe the arc-melt pool behavior. Hongkun *et al.* [3] summarized and analyzed various GTAW (Gas Tungsten Are Welding) coupled numerical simulation models. Pengfei [4] conducted multimethod research on magnetic fluids through numerical simulation methods to provide technical and theoretical support for the development and application of high-performance magnetic fluids. Kong *et al.* [5] improved the ocean model through a variety of numerical simulation methods to study the diffusion of organisms in more complex ocean regions. Guoping and Mengxiao [6] used the finite difference program in numerical simulation to study the pile-soil interaction of the oblique and orthogonal pile foundations. These studies have carried out simulation studies on many aspects of engineering problems such as liquids, oil fields, electric power and even problems in a wide range of oceans, but they are all analyzed from a macro perspective, and there are still some problems that lack a certain microscopic explanation.

The associate editor coordinating the review of this manuscript and approving it for publication was Yizhang Jiang.

From a microscopic point of view, Qingyan *et al.* [7] simulated superalloy blades under different processes and compared and analyzed their microstructure evolution law. Based on the mechanism of microbial flooding, Tianyuan *et al.* [8] introduced and summarized the research status of the numerical simulation of microbial flooding from two aspects: a mathematical model and a software application. Pei *et al.* [9] summarized the results of various theoretical studies on the grouting problem of actual engineering and discussed the breakthrough progress of numerical simulation of mesomechanics, which can provide reference and inspiration for the development of grouting technology in underground engineering. Bo [10] summarized a variety of advanced numerical simulation methods for studying multifield coupled rocks and compared them with macroscopic methods. These scholars have carried out more detailed microscopic studies on various engineering problems such as alloy, oil recovery, grouting, engineering rock mass, etc., and explained the problems that are difficult to be explained from the macroscopic perspective at a deeper level. Although the computer numerical simulation method has made some progress in many aspects, the problems in practical engineering are complicated, and a simple computer numerical simulation study may not be able to solve practical problems. Therefore, the research results need to be applied to practical engineering to verify their correctness.

In practical engineering applications, Zhang *et al.* [11] used finite element numerical models to predict the dynamic response of long-span bridges, applied them to practical problems, and achieved good results. Cao *et al.* [12] further optimized the finite element numerical simulation method and changed the piezoelectric impedance/admittance sensing used for structural health monitoring, and the actual test results verified the correctness of the method. Barcena *et al.* [13] studied and verified wind technology through numerical simulation methods and truly reproduced the 5 MW wind of the National Renewable Energy Laboratory (NREL) high-performance turbine. Li *et al.* [14] combined different numerical simulation algorithms to study the relationship between in-situ stress and rock in actual engineering, and achieved good agreement with actual observation results. The above research has solved many problems in actual construction projects through a variety of different numerical simulation software, but these are almost all problems above the ground. Due to the resource needs such as metal mines and coal mines, mining projects for mineral resources are gradually shifting to deeper depths underground. In deep underground mine engineering, the depth is as great as hundreds or even thousands of meters. The greater higher depth makes this geological environment much more complicated than ground engineering. If effective measures are not taken, then engineering safety will be seriously affected. Regarding this type of issue, relevant scholars have performed some research. Wu *et al.* [15] used the FDS numerical simulation method to study the changes in mine tunnels at different temperatures, and their research was highly consistent with the measured results. Chang *et al.* [16] combined the FDTD numerical simulation method with the TEM method to detect the water-rich regions around a mine roadway. The main problem that directly affects engineering safety is the large displacement of the roadway and the difficulty of supporting it. Although these studies have conducted a certain analysis of the geological environment, they still cannot solve this problem. While there have been some mature support schemes in the construction of other mines, due to the complexity and difference of geological conditions, specific support schemes cannot be simply copied. In actual projects, many factors such as costs and support effect need to be considered, and the proposed support plan cannot be tested multiple times. Therefore, the problem of designing a reasonable support plan has taken on renewed urgency. Accordingly, it is necessary to propose an effective support scheme for deep underground engineering through computer numerical simulation software combined with reasonable methods.

Therefore, this article combined FLAC^{3D} software and the PDM method to design and optimize the support scheme of a mine tunnel with a depth of 850 m in Hebei Province and has achieved good results in actual engineering. The roadway displacement obtained by the research of this article is basically consistent with the actual monitoring value in the law and is also close in value. This fully proves the reliability of the research in this article and provides effective guidance and reference for engineering problems in the region under similar geological conditions.

II. NUMERICAL MODEL AND CALCULATION PARAMETERS

To study the surrounding rock displacement of the roadway and choose a more suitable roadway support scheme to ensure the normal progress of the construction, a numerical calculation model of the actual situation of a certain project was established.

A. BASIC ASSUMPTIONS AND SURROUNDING ROCK PARAMETERS

In the process of numerical analysis, to facilitate the calculation and improve calculation efficiency, the actual working conditions are processed without greatly reducing the accuracy. That is to say, the key factors are primarily considered, and some non-key factors or relatively minor factors are simplified and ignored. Therefore, the following assumptions are proposed before the numerical simulation analysis:

(a) The surrounding rock of the roadway is homogeneous and isotropic;

(b) Since the roadway is deeply buried, the initial stress of the surrounding rock consists of self-weight stress and tectonic stress. The gravity of the overlying rock layer is considered by applying equivalent surface stresses, and the lateral pressure coefficient is used to simulate deep rock mass stress;

(c) The effect of grouting reinforcement is considered through the principle of equivalence, that is, the mechanical

TABLE 1. Physical and mechanical parameters of surrounding rock.

Rock	Elasticity modulus (E/MPa)	Poisson ratio (μ)	Unit weight (γ /kN • m^{-3})	Cohesion (c/MPa)	Friction angle (φ /°)	Tensile strength ($Tens$/MPa)
Siltstone	12.1×10^3	0.23	26.7	9.6	37	6.8
Sandy mudstone	4.10×10^3	0.30	25.8	1.7	28	3.5
Argillaceous siltstone	6.20×10^3	0.25	26.1	4.5	31	5.2

parameters of the rock formation in the region of anchor grouting reinforcement are improved, and the extent of improvement must be determined through laboratory tests;

(d) To consider the support effect of the metal mesh, the elastic modulus of the metal mesh is converted to that of shotcrete lining based on the principle of equivalence, and the elastic modulus E of the shotcrete lining is equivalently considered.

The rock formations in this project are siltstone, sandy mudstone, and argillaceous siltstone. Based on on-site investigation, a mechanical parameter test and geological exploration report, combined with the rock mass quality classification system, the rock mass quality grade was determined. Through indoor petrophysical tests on the sampled rocks, physical and mechanical parameters, such as the uniaxial compressive strength, are obtained. The mechanical parameters of the shotcrete lining are determined by engineering analogy. The physical and mechanical parameters of the surrounding rock are manifested in Table 1. The shotcrete lining in this article adopts the concrete with an elastic modulus of 2.55 × 104 MPa, a Poisson's ratio of 0.2, a strength of C20, and a shotcrete lining thickness of 120 mm.

B. ESTABLISHMENT OF THE NUMERICAL MODEL

FLAC^{3D} is an extension of the two-dimensional finite difference program FLAC^{2D} that which can simulate the force characteristics and plastic flow analysis of the three-dimensional structure of soil, rock and other materials. The program fits the actual structure by adjusting the polyhedral elements in the three-dimensional grid. The element material can adopt the linear or nonlinear constitutive model. Under the action of external force, when the material yields and flows, the mesh can deform and move accordingly (large deformation mode). FLAC^{3D} adopts the explicit Lagrangian algorithm and hybrid-discrete partitioning technology, which can simulate the plastic failure and flow of materials very accurately. FLAC^{3D} has the following advantages:

1) The ''hybrid-discrete method'' is used to simulate plastic failure and plastic flow. This method is more accurate and reasonable than the ''discrete integration method'' usually used in the finite element method.

2) Even if the simulated system is static, the dynamic equation of motion is still used, which ensures that FLAC^{3D} does not encounter numerical obstacles in simulating the unstable process of physics.

3) An ''explicit solution'' scheme is adopted. Therefore, the time it takes for the explicit solution to solve the nonlinear stress-strain relationship is almost the same as the linear constitutive relationship, whereas the implicit solution will take a longer time to solve the nonlinear problem. Moreover, it is not necessary to store the stiffness matrix, which means that the use of medium-capacity memory can solve the multiunit structure; the simulation of large deformation problems hardly consumes more calculation time than small deformation problems because there is no stiffness matrix to be modify [17].

Du *et al.* [18] proposed a solution to the precracking of a roof of an abandoned roadway by aiming at the problem of how the abandoned roadway in the roadway excavation affects the normal roadway work. FLAC^{3D} numerical software was used to calculate the vertical stress and vertical displacement of the roof under different roof precracking distances. Analyzed and carried out engineering application, and achieved good results. The research results provide a theoretical basis for how to support the roadway during driving. Zhu *et al.* [19] used FLAC^{3D} software to build a rock mass model for goaf support and compaction to simulate the failure characteristics of surrounding rock during goaf pressure relief and equipment extraction. A comprehensive evaluation of the surrounding rock control effects of different support schemes and mining schemes was performed. The results show that the combination of improved support design and equipment bidirectional drainage has the best surrounding rock control effect. Yuan *et al.* [20] studied the clarification of the influence of anchor bolts on the support of a layered weak roof and surrounding rock. FLAC^{3D} was used to establish a roadway mechanical model of a nonlayered homogeneous roof and a layered weak roof. The distribution characteristics of the stress field and displacement field of the bolt support were analyzed, and the effect of the bolt support on the roof of two roadways was studied. HaiTao *et al.* [21] used FLAC^{3D} numerical software to simulate a rectangular cross-section support form composed of bolts, anchor cables, and anchor nets. The simulation results and field applications show that the improved support form can more effectively control the two ribs and the ground

uplift. And better solve the greater deformation that occurs in the return air. In summary, FLAC^{3D} software can effectively solve roadway support problems. Therefore, the software is selected for numerical simulation in this article.

FLAC^{3D} numerical simulation software is used to establish the roadway model. The model size is 80 × 80 × 30 m (length × height × width). To reduce the error caused by the size of the model and improve the calculation efficiency, the model is built with 5 times the roadway diameter as the boundary. In the modeling process, the bottom of the model is set as a fixed boundary, and the top of the model is controlled by stress boundary conditions. In addition, the excavation area of the roadway is controlled by stress boundary conditions and displacement boundary conditions, and the static calculation end boundary imposes horizontal speed constraints. According to the actual engineering geological conditions of the mine roadway, the average weight of the overlying rock layer is $\gamma = 24$ kN/m^3. The roadway is buried at a depth of 850 m, the load value of the overlying rock layer acting on the roadway is 19.44 MPa, and the roadway model is shown in Figure 1. L1 - L9 refer to the different layering of mudstone, sandy mudstone and siltstone. The model is based on the stratification of rock mass in actual geological conditions. The difference in color only distinguishes only the adjacent layers of rock and has no special meaning.

Simulation steps:

Step 1: Excavate the roadway part step by step according to the project requirements.

Step 2: After excavation, support shall be carried out according to the designed corresponding support scheme.

Step 3: Record the relevant numerical changes of the roadway: maximum and minimum principal stresses; vertical and horizontal displacements; and displacement and stress of the support structure.

Step 4: Arrange certain measuring points according to the required requirements for displacement monitoring.

Step 5: Carry out certain parameter optimization according to the required requirements, and repeat the above steps.

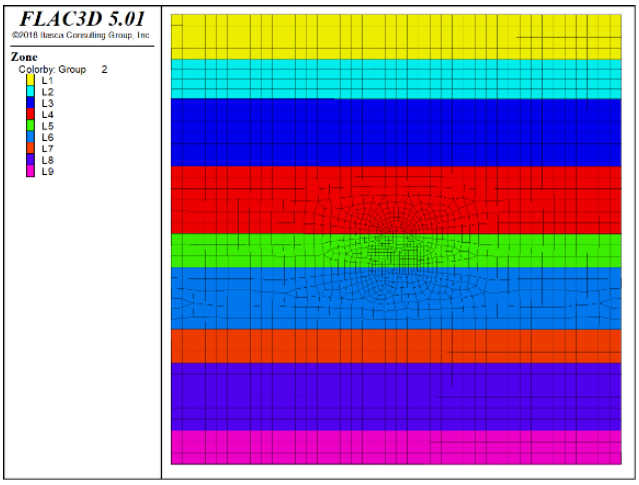

(a) The sketch of the model surrounding rock layers

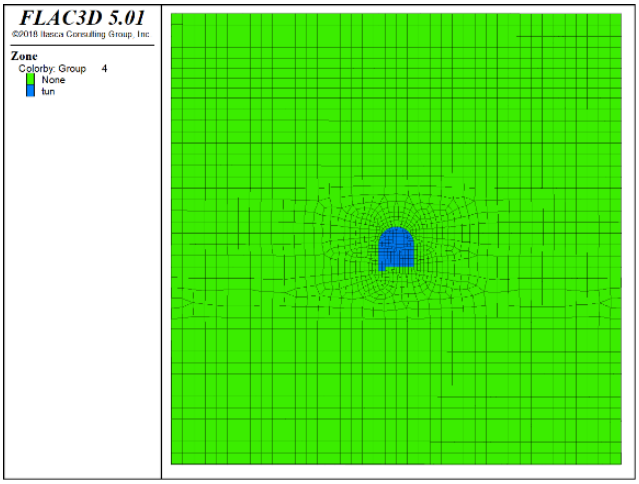

(b) The sketch of the position of the roadway in the model

FIGURE 1. Model diagram of the roadway and surrounding rock.

III. INITIAL SUPPORT SCHEME AND NUMERICAL SIMULATION ANALYSIS OF ROADWAY

After the roadway was excavated in accordance with the design requirements, no support measures were taken at this time. Numerical simulation analysis was performed for the stress and displacement of the roadway at this time.

A. NUMERICAL SIMULATION ANALYSIS OF THE ROADWAY WITHOUT SUPPORT

The roadway excavation is simulated, and the FLAC^{3D} numerical simulation results after external stress balance are displayed in Figure 2 and Figure 3.

1) STRESS FIELD ANALYSIS

Figure 2 shows that when the roadway is excavated without support measures, the maximum tensile stress on the floor is 2.95 MPa. There is a larger stress area at the roof and floor of the roadway, while the stress area of the two roadway walls is smaller.

2) DISPLACEMENT FIELD ANALYSIS

The vertical displacement and horizontal displacement are primarily analyzed after external stress balance.

After the excavation of the roadway, the surrounding rock displacement is obvious, the horizontal displacement occurs on the two roadway walls, and the vertical displacement primarily occurs on the roof and floor. Among these displacements, the maximum displacement of the floor is at the center of the floor. It reaches 494 mm, indicating that the roadway floor is severely damaged. The horizontal displacements of the two roadway walls are roughly identical, approximately 150 mm, as shown in Figure 3.

Therefore, if the roadway is not supported in time after excavation, the surrounding rock of the roadway will deform under the action of the surrounding rock pressure, and the amount of displacement will increase rapidly, which will easily cause phenomena manifested as falling roofs and

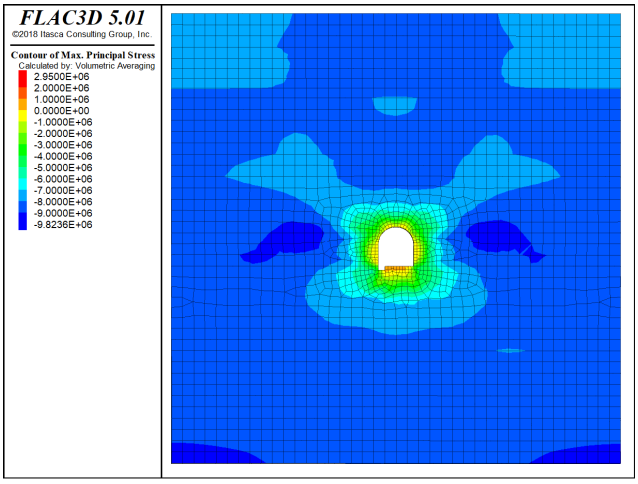

(a) Cloud diagram of the maximum principal stress

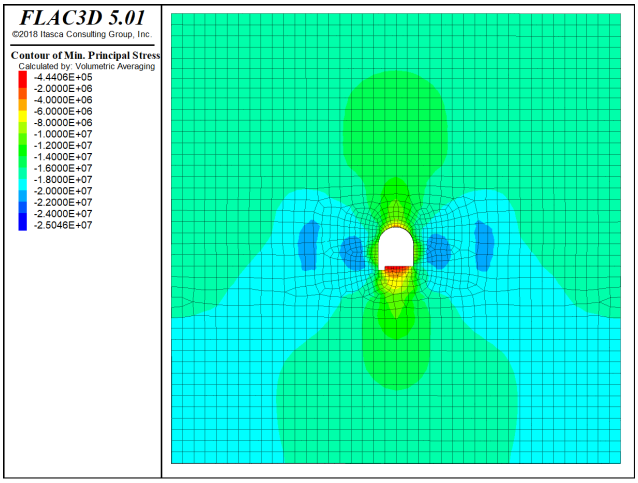

(b) Cloud diagram of the minimum principal stress

FIGURE 2. The cloud diagram of the principal stress without support.

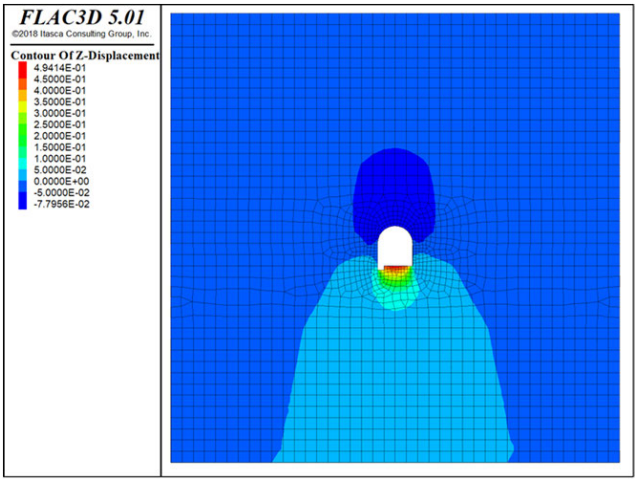

(a) Cloud diagram of the vertical displacement

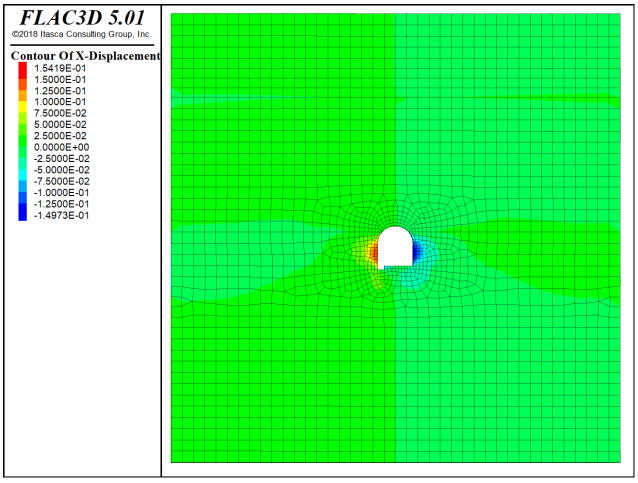

(b) Cloud diagram of the horizontal displacement

FIGURE 3. Cloud diagram of the displacement without support.

heaving floors. This result will greatly affect the personal and property safety of the staff in the roadway.

B. INITIAL SUPPORT SCHEME FOR THE ROADWAY

1) THE ROADWAY SUPPORT OF THE ROOF AND TWO ROADWAY WALLS

The main support measure is a combination of the anchor net spray and the grouting of the surrounding rock. During the construction of the roadway, the main structure of the primary support is the anchor net spray, and a steel ladder is used to connect the bolts. To increase the restraining stress of the anchor cable on the surrounding rock of the roof and two roadway walls, a T-shaped steel belt is selected as the anchor cable support tray. Metal mesh is arranged on the surface of the surrounding rock of the roof and two roadway walls, and concrete is sprayed in time after the laying is completed to enhance the active support of the surrounding rock of the roof and two roadway walls and thus prevent instability.

2) THE ROADWAY SUPPORT OF THE FLOOR SUPPORT

The initial support scheme only applies only four bolts to the floor of the roadway for support and reinforcement. The sketch of the initial support scheme is exhibited in Figure 4.

The specific contents of the initial support scheme are as follows:

(a) Anchor cables: a total of 9 anchor cables are arranged, the specification of each anchor cable is $\Phi 17.8 \times 8500$ mm, and the row spacing between anchor cables is 1600 mm. The measured anchorage length should be greater than 2000 mm, and the anchoring stress should not be less than 250 kN. The initial anchoring stress is not less than 150 kN.

(b) Bolts: high-strength prestressed bolts are selected. The specification of each bolt is $\Phi 22 \times 2400$ mm, and the row spacing between bolts is 800 mm. The measured anchorage length should be greater than 1000 mm, and the anchoring stress should not be less than 150 kN. The anchor stress is not less than 50 kN, otherwise it should be adjusted.

(c) Bolts on the floor: high-strength prestressed bolts are selected. The specification of each bolt is $\Phi 22 \times 2400$ mm,

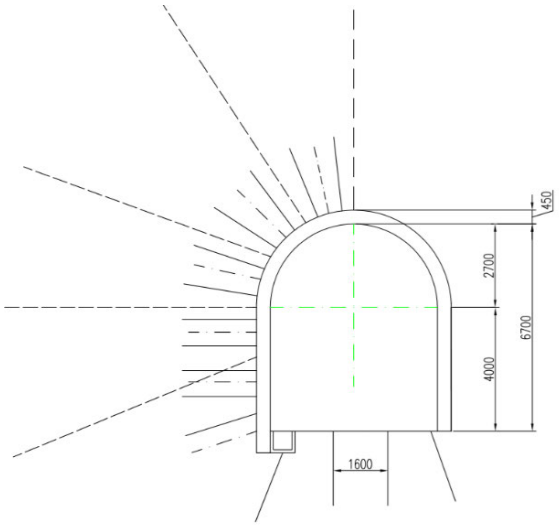

FIGURE 4. Sketch of the initial support scheme.

and the row spacing between floor bolts is 1600 mm. The anchoring stress is not less than 150 kN, and the initial anchoring stress is not less than 50 kN.

(d) Grouting bolts: they are made of seamless steel pipe. The specification of each grouting bolt is $\Phi 25 \times 2200$ mm, and the row spacing between grouting bolts is 1600 mm to ensure the grouting range to enhance the overall strength of the surrounding rock.

(e) Metal mesh: it is made of round steel spot welding. The round steel diameter is $\Phi 6.5$ mm, the specification of each metal mesh is 1100×2100 mm, and the mesh size of the metal mesh is 100×100 mm.

(f) Shotcrete lining: the strength of concrete is C20, the ratio is 1:2:2, and the thickness of the sprayed layer is 120 mm.

C. NUMERICAL SIMULATION ANALYSIS OF THE INITIAL SUPPORT SCHEME

1) STRESS FIELD ANALYSIS

The maximum tensile stress on the floor is 2.65 MPa (Figure 5). After adopting the initial support scheme, compared with the state of the roadway without support (III A), the stress value of the roadway floor is reduced, but there is a certain stress concentration in the two roadway walls and roof. In addition, there is obvious stress concentration in a certain range under the roadway floor. If the floor is not reinforced, floor heave will occur, which will affect the normal production of the coal mine.

2) DISPLACEMENT FIELD ANALYSIS

The maximum displacement in the roadway occurs in the floor, with a maximum value of 359 mm. As the depth increases, the displacement gradually stabilizes. Compared with the state of the roadway without support (III A), the roof displacement decreased from 78 mm to 60 mm, and the displacement of the floor heave decreased from 494 mm to 359 mm (Figure 6).

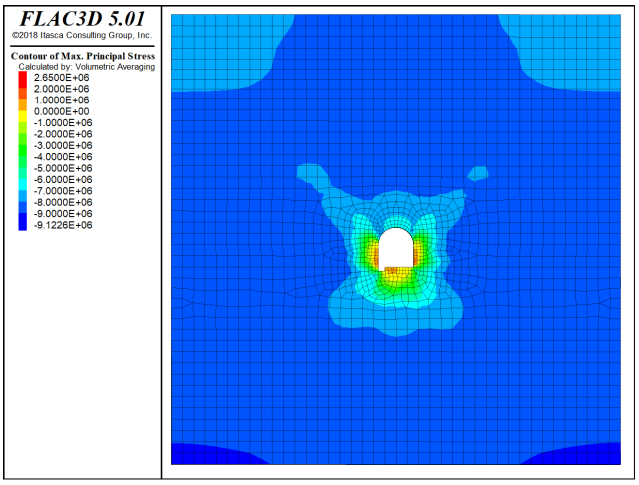

(a) Cloud diagram of the maximum principal stress

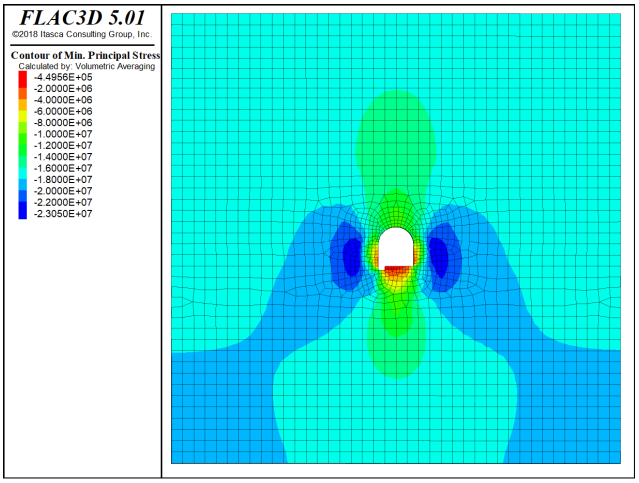

(b) Cloud diagram of the minimum principal stress

FIGURE 5. Cloud diagram of the principal stress with the initial support scheme.

Although the amount of displacement of the surrounding rock has been reduced, the extent of the decrease is not obvious. Under such supporting conditions, the displacement of floor heave produced remains large, and the roadway cannot meet the normal production standards. Therefore, it is necessary to propose a new roadway support scheme.

3) ANALYSIS OF THE SUPPORTING STRUCTURE

(a) Displacement: when using the initial support plan to reinforce the roadway, the maximum displacement of the anchor cable in the support structure is generated on the two roadway walls. The maximum displacement of the bolts is generated on the roadway floor, and the maximum displacement is 166 mm (Figure 7(a)).

(b) Stress: in terms of the stress on the supporting structure, the stress is greater in the middle of the bolts than at the two ends. On the whole, the stress is smaller on the left roadway wall than on the right roadway wall (Figure 7(b)).

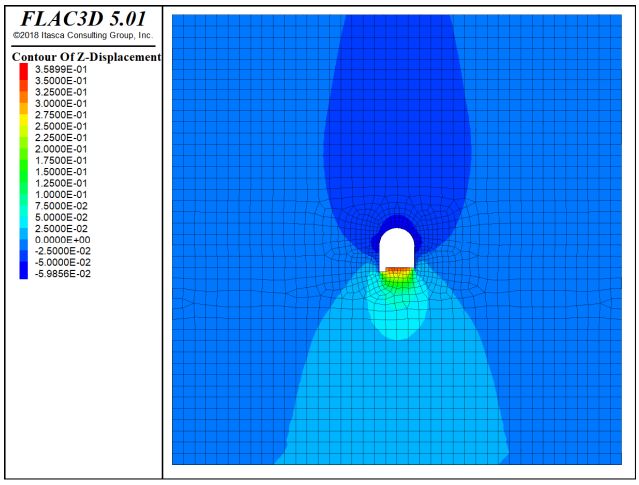

(a) Cloud diagram of the vertical displacement

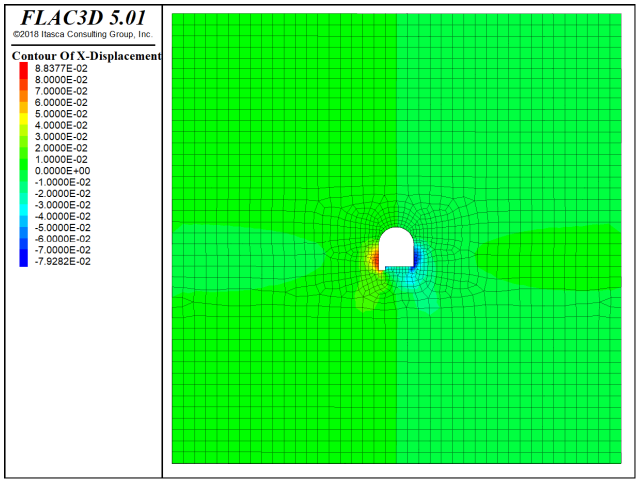

(b) Cloud diagram of the horizontal displacement

FIGURE 6. **The cloud diagram of the displacement with the initial support scheme.**

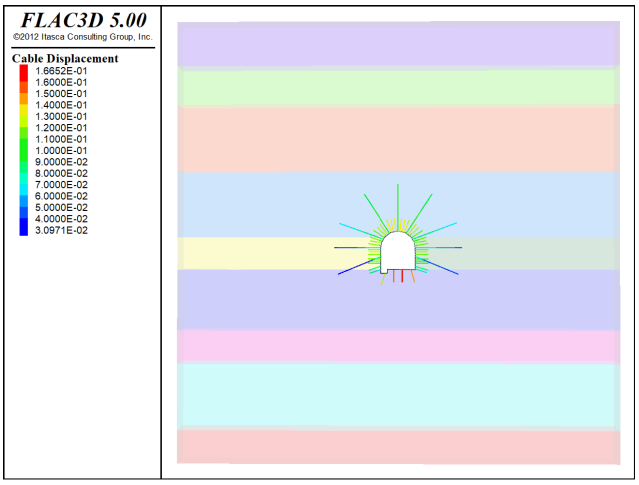

(a) Cloud diagram of the displacement

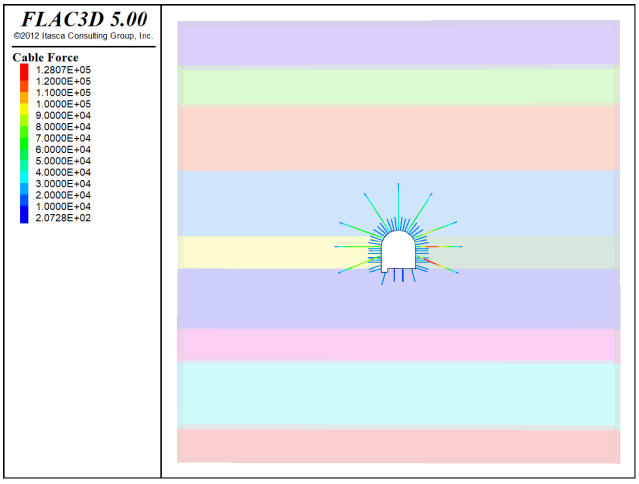

(b) Cloud diagram of the stress

FIGURE 7. **Cloud diagram of the displacement and stress of the supporting structure.**

IV. NUMERICAL SIMULATION ANALYSIS OF THE NEW ROADWAY SUPPORT SCHEME

A. PROPOSAL OF THE NEW ROADWAY SUPPORT SCHEME

In the initial support scheme of the coal mine roadway, the combined support method of the anchor net spray and grouting adopted in the roof and the two roadway walls of the roadway is a more commonly used and mature support method with high support strength. In addition, through reference to the design of other roadway support schemes in the mine, it is determined that the roof and the two roadway walls of the roadway will continue to adopt the support form of the anchor net spray and grouting.

From the previous analysis, it is seen that the part with greater displacement of the roadway is the floor. In other common mine roadway constructions, the floor is also the part of the roadway that is most prone to large displacement, which is consistent with the previous analysis results. In addition, floor reinforcement is the most difficult part of roadway support and is often referred to as the floor heave problem.

Progressive design method (PDM): Because the design scheme needs to comprehensively consider cost, rational use of resources and other factors but is subject to the unknowns of the actual effect of the scheme, it is necessary to gradually optimize the known conventional scheme and analyze its feasibility to find the best answer.

Through the field investigation of the coal mine, combined with the analysis of the relevant geological conditions and survey data, it is determined that the roadway floor heave is a stress type floor heave. To better suppress the occurrence of the floor heave phenomenon, the floor heave control mechanism is analyzed, and the floor heave control methods at home and abroad are summarized. Combined with the actual engineering situation of the roadway, on the basis of keeping the roof and the two roadway walls of the roadway support scheme unchanged, PDM is used to design the roadway floor reinforcement, and three new roadway support schemes are proposed primarily for the floor heave problem:

New roadway support scheme 1: Floor bolts (increase the layout density of floor bolts, from four bolts in the initial roadway support scheme to eight bolts);

New roadway support scheme 2: Floor bolts and grouting;

New roadway support scheme 3: Floor bolts and grouting and prestressed anchor cable bundle.

Figure 8 is a sketch of the new roadway support schemes. The relevant parameters of the roof and the two roadway walls of the roadway support material are identical to those of the initial support scheme. The relevant parameters of the roadway floor support materials are as follows:

(1) Floor bolts: adopt high-strength prestressed bolts, and the specification of each bolt is $\Phi 22 \times 2400$ mm;

(2) Floor grouting bolts: 4 floor grouting bolts are arranged in each section and at intervals from the anchor cables, with a specification of $\Phi 25 \times 1400$ mm;

(3) Floor anchor cable bundle: one anchor cable is arranged in the center of the floor, and three anchor cables are arranged in each section on the floor. The specification of the anchor cable is $\Phi 17.8 \times 8500$ mm.

B. NUMERICAL SIMULATION ANALYSIS OF THREE NEW ROADWAY SUPPORT SCHEMES

After the excavation of the roadway, for three different roadway support schemes, the changes in the roadway stress field (including the maximum principal stress and the minimum principal stress), the displacement field analysis (including the vertical displacement and the horizontal displacement), and the support structure (stress and displacement) were subjected to comparative analysis.

1) NEW ROADWAY SUPPORT SCHEME 1: FLOOR BOLTS

a: STRESS FIELD ANALYSIS

After the roadway was supported, the maximum tensile stress on the floor was reduced from 2.65 MPa under the initial support scheme to 1.85 MPa. The stress concentration area near the two roadway walls of the roadway has been reduced, and the stress concentration phenomenon has been improved (Figure 9).

b: DISPLACEMENT FIELD ANALYSIS

After the floor bolts are used to reinforce the roadway, the maximum floor heave amount is 275 mm. Compared with the two cases in which no supporting measures are taken and the initial support scheme is adopted, the heave amount is reduced by 219 mm and 84 mm, respectively. The displacement of the two roadway walls of the roadway has also decreased. Although support scheme 1 can restrain the displacement of the floor to a certain extent, considering the long-term production and operation of the coal mine, the effect of single-use floor bolt support is not ideal (Figure 10).

c: ANALYSIS OF SUPPORTING STRUCTURE

After increasing the number of floor bolts, the displacement of the floor bolts near the center of the floor is the largest, and the displacement of the bolts on the two roadway walls of the roadway is reduced compared with that of the initial support scheme. On the other hand, the stress value of each bolt is reduced, the supporting structure is evenly stressed, and the stress is greater in the middle of the bolts than at the two ends. Overall, the stress is smaller

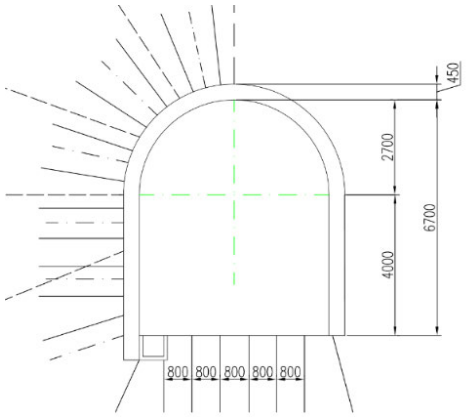

(a) New roadway support scheme 1

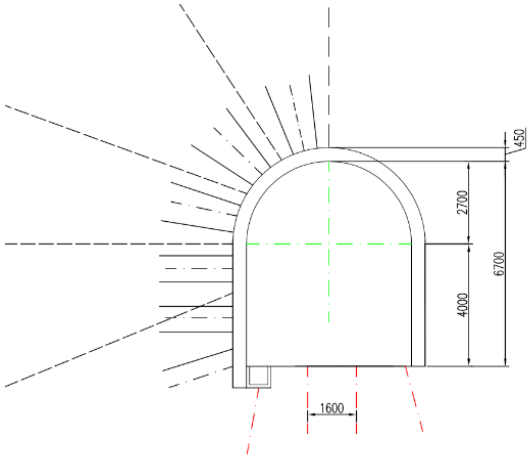

(b) New roadway support scheme 2

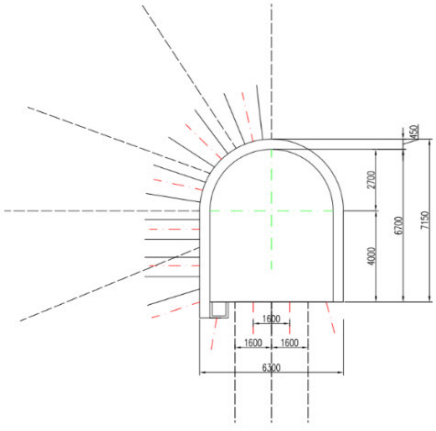

(c) New roadway support scheme 3

FIGURE 8. Sketch of the new roadway support schemes.

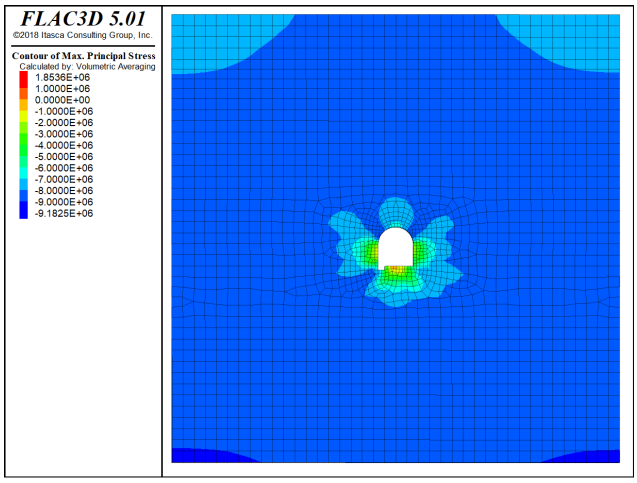

(a) Cloud diagram of the maximum principal stress

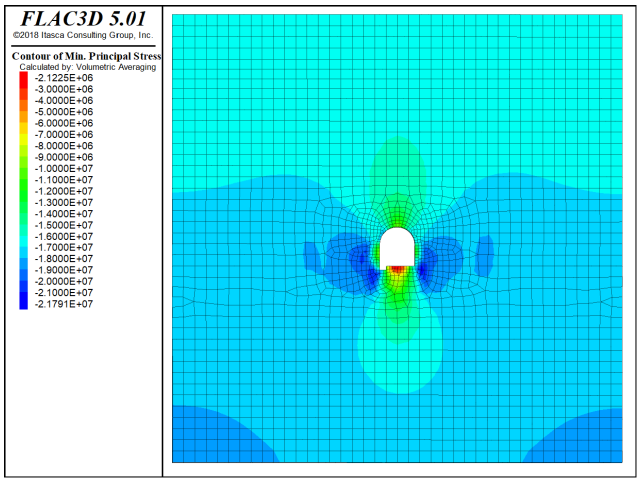

(b) Cloud diagram of the minimum principal stress

FIGURE 9. Cloud diagram of the principal stress with new roadway support scheme 1: floor bolts.

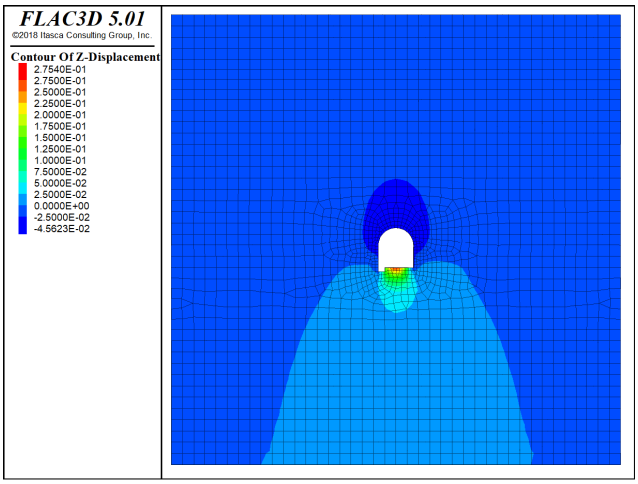

(a) Cloud diagram of the vertical displacement

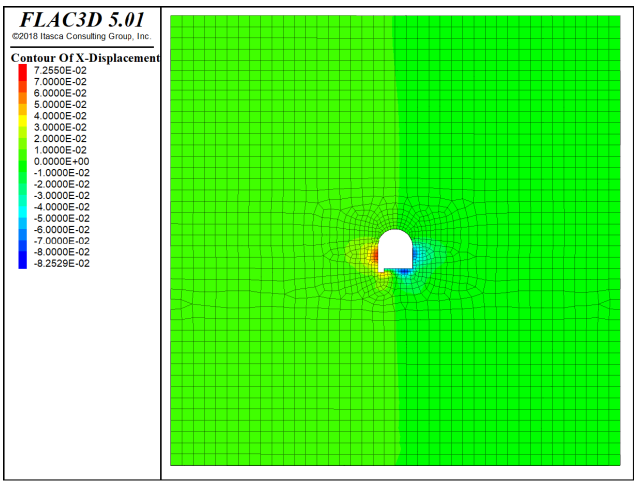

(b) Cloud diagram of the horizontal displacement

FIGURE 10. Cloud diagram of the displacement with new roadway support scheme 1: floor bolts.

on the left side supporting structure than on the right side (Figure 11).

2) NEW ROADWAY SUPPORT SCHEME 2: FLOOR BOLTS AND GROUTING

a: STRESS FIELD ANALYSIS

After the floor bolts and grouting are arranged on the floor, the maximum tensile stress value at the roadway floor is reduced from 2.65 MPa in the case of supporting only the roof and the two roadway walls of the roadway to 1.68 MPa. Compared with the stress value when the floor bolt (scheme 1) is used for reinforcement, there is a slight change. The stress concentration area near the two roadway walls of the roadway has been reduced, and the stress concentration phenomenon has been weakened compared with that of scheme 1. Through floor bolts and grouting, the development of the cracks in the surrounding rock of the roadway floor is effectively restrained, the integrity of the rock mass around the roadway floor is improved, the overall strength of the rock mass is increased, and the stress concentration phenomenon of the roadway floor is improved (Figure 12).

b: DISPLACEMENT FIELD ANALYSIS

After using floor bolts and grouting to reinforce the roadway floor, the maximum floor heave is 185 mm. Compared with support scheme 1, the floor heave is reduced by 90 mm, and the displacement of the two roadway walls of the roadway is further reduced. Although support scheme 2 can restrain the displacement of the floor to a certain extent, the amount of floor heave remains large, and the effect of the single use of the floor bolts and grouting support is not ideal (Figure 13).

c: ANALYSIS OF SUPPORTING STRUCTURE

Because of the increase in supporting strength, compared with that of support scheme 1, the maximum displacement of the bolts has been reduced, and the displacement of the supporting structure in the roof and two roadway walls of the roadway have changed significantly. On the other hand,

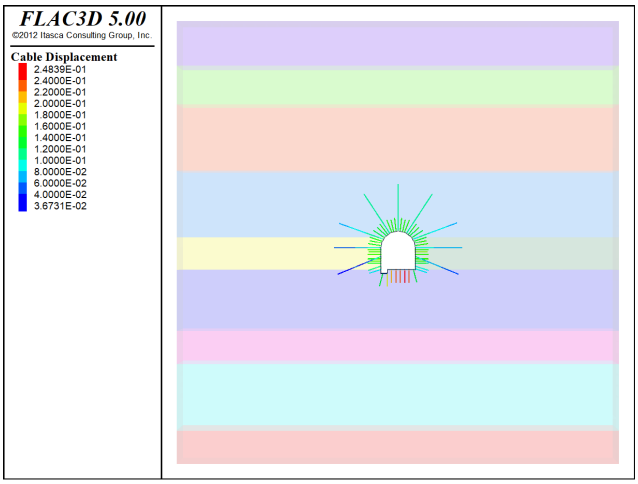

(a) Cloud diagram of the displacement

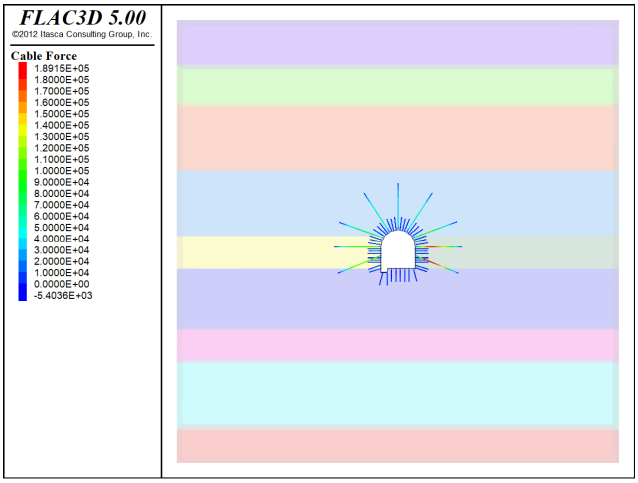

(b) Cloud diagram of the stress

FIGURE 11. Cloud diagram of the displacement and stress of the supporting structure.

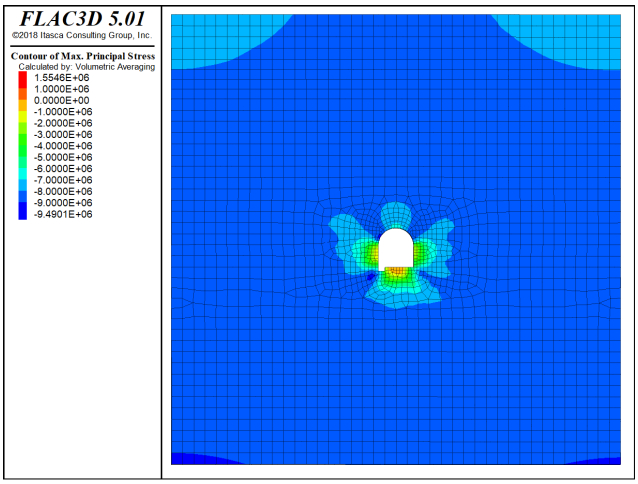

(a) Cloud diagram of the maximum principal stress

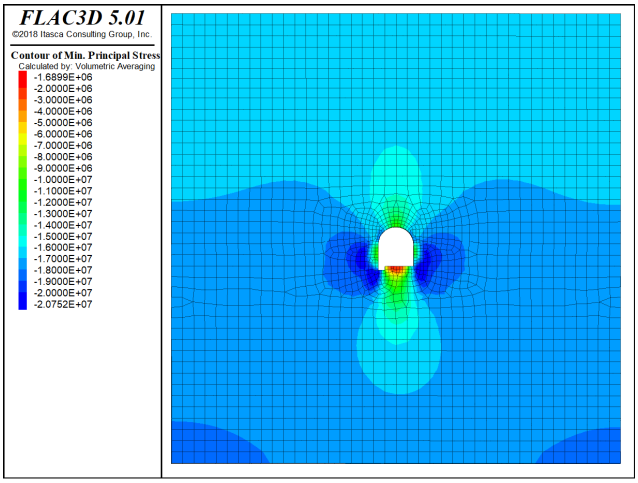

(b) Cloud diagram of the minimum principal stress

FIGURE 12. Cloud diagram of the principal stress with new roadway support scheme 2: floor bolts and grouting.

the maximum stress value of the bolts is further reduced, and the stress range in the middle of each bolt is increased. Overall, the stress of the left side support structure remains smaller than that of the right side (Figure 14).

3) NEW ROADWAY SUPPORT SCHEME 3: FLOOR BOLTS AND GROUTING AND PRESTRESSED ANCHOR CABLE BUNDLE

a: STRESS FIELD ANALYSIS

After adopting the combination support scheme of scheme 3, the stress concentration degree and range of the roadway surrounding rock are significantly reduced compared with those of support schemes 1 and 2, and only part of the stress concentration remains at the bottom corner. Within a certain depth range under the floor, the stress concentration phenomenon is obviously improved, and the stress value is greatly reduced compared with those of schemes 1 and 2. The maximum tensile stress at the floor of the roadway was reduced from 2.95 MPa to 0.54 MPa, a decrease of 81.7%. Through the analysis of the simulation results, it is also fully proven that the floor anchor cable bundles have a good weakening effect on the stress concentration of the surrounding rock on the floor. The floor anchor cable bundles share part of the ground stress that should be borne by the surrounding rock of the roadway, so that the surrounding rock stress on the surface of the roadway floor is transferred deeper (Figure 15).

b: DISPLACEMENT FIELD ANALYSIS

After the floor bolts are used to reinforce the roadway, the maximum floor heave amount is 275 mm. Compared with the unsupported case, the floor heave amount is reduced by 448 mm. In addition, compared with the case where only the roof and the two roadway walls of the roadway are supported, the floor heave is reduced by 313 mm. In contrast, the displacement of the floor heave of scheme 3 is 229 mm and 139 mm less than that of the scheme 1 and scheme 2, respectively, and the floor heave amount is significantly reduced. Therefore, through numerical analysis, it is known that this support scheme can play a considerable role in supporting the roadway floor, greatly reducing the amount of floor heave,

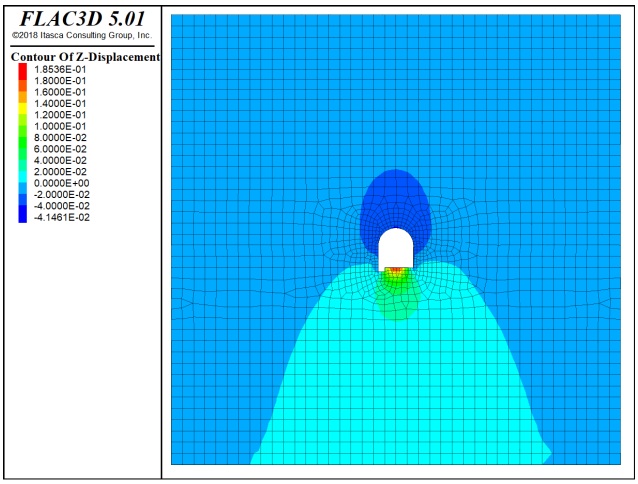

(a) Cloud diagram of the vertical displacement

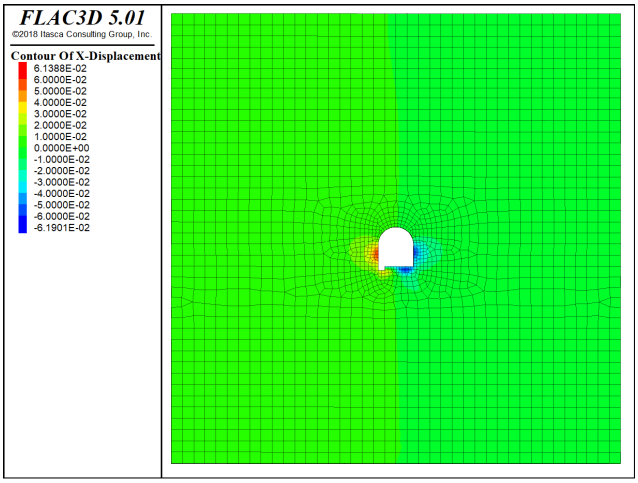

(b) Cloud diagram of the horizontal displacement

FIGURE 13. The cloud diagram of the displacement with new roadway support scheme 2: floor bolts and grouting.

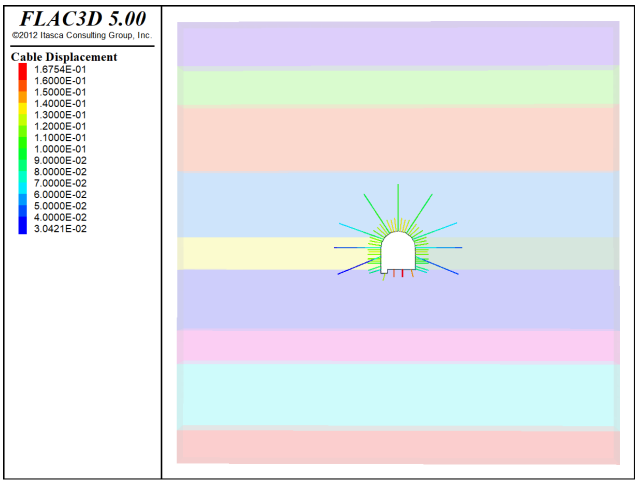

(a) Cloud diagram of the displacement

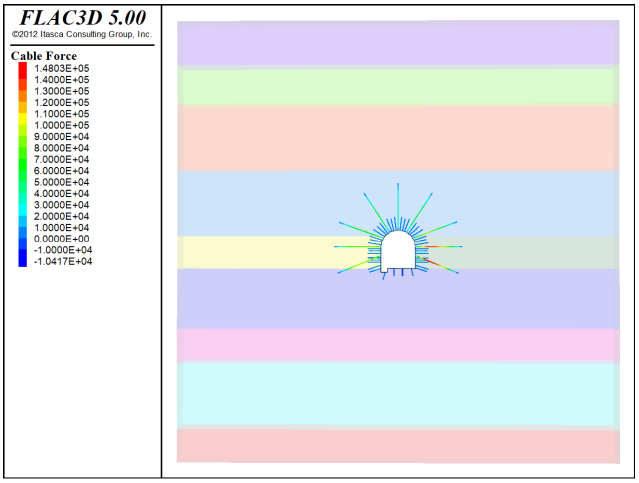

(b) Cloud diagram of the stress

FIGURE 14. Cloud diagram of the displacement and stress of the supporting structure.

and the treatment effect has reached the standard for safe production (Figure 16).

c: ANALYSIS OF SUPPORTING STRUCTURE

After adopting the combination support scheme of scheme 3, the maximum displacement of the bolts is located at the roof of the roadway. Because of the addition of the floor anchor cable bundle, the stress of the surrounding rock is transmitted deeper, and the displacement of the floor bolt is significantly reduced compared with those of schemes 1 and 2. In terms of stress, because of the addition of prestressed anchor cable bundles in the floor, the stress distribution around the roadway is more uniform, and the stress concentration is significantly reduced. The stress value of the bolts is also reduced, and the stress of the supporting structure is more uniform.

4) ANALYSIS OF THE DISPLACEMENT OF FLOOR HEAVE ON THE ROADWAY FLOOR

Through the analysis of the displacement cloud diagram above, it is known that the maximum displacement of the roadway floor is located near the center of the floor. To effectively analyze the displacement of the roadway floor under different support schemes, the monitoring variable function of FLAC^{3D} software is used, so the measuring hole is arranged in the center of the floor. For displacement monitoring in the axial direction, the monitoring positions are 3 m, 6 m and 10 m below the floor of the roadway centerline, and the corresponding measuring points are numbered 501, 502 and 503, respectively. Generally, the system defaults to record a value every 10 iterations, and the monitoring results are shown in Figure 18.

In the depth range of 0-10 m under the floor of the roadway, when the roadway floor is reinforced by the floor bolts and grouting and prestressed anchor cable bundle (support scheme 3), the deep displacement of the floor is reduced to varying degrees compared with those of support schemes 1 and 2, especially in the range of 0-6 m, and the decrease is very obvious. In the range of 6-10 m, the decline in the displacement value becomes gradual.

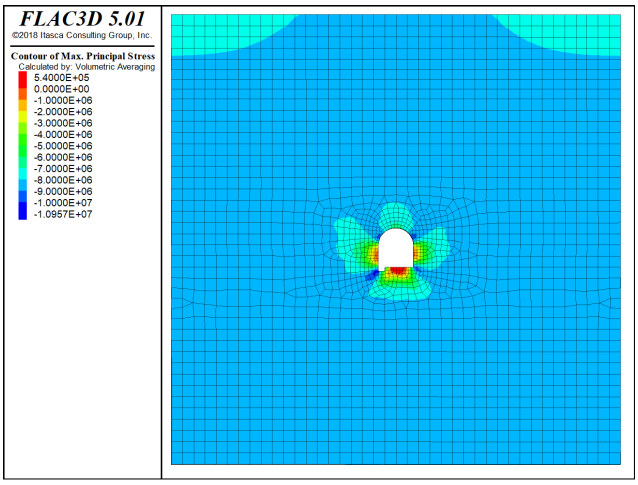

(a) Cloud diagram of the maximum principal stress

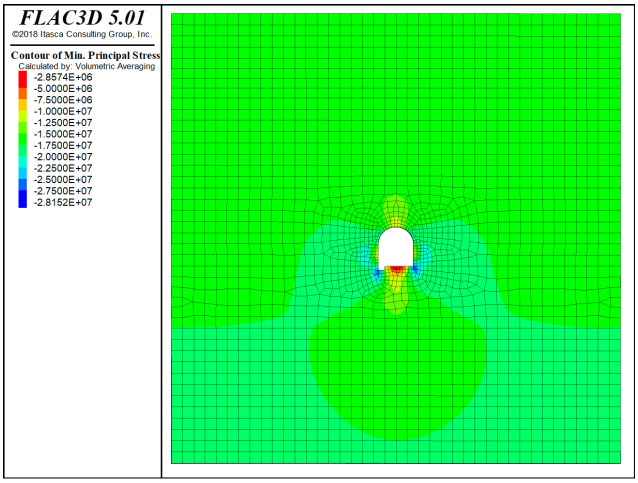

(b) Cloud diagram of the minimum principal stress

FIGURE 15. Cloud diagram of the principal stress with new roadway support scheme 3: floor bolts and grouting and prestressed anchor cable bundle.

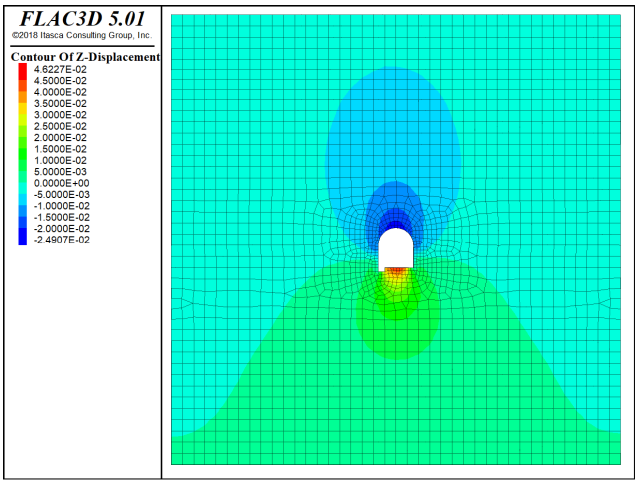

(a) Cloud diagram of the vertical displacement

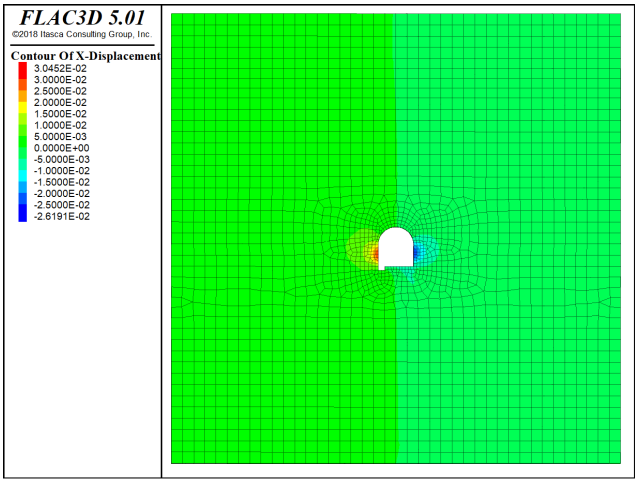

(b) Cloud diagram of the horizontal displacement

FIGURE 16. Cloud diagram of the displacement with new roadway support scheme 3: floor bolts and grouting and prestressed anchor cable bundle.

In summary, the floor bolts and grouting and prestressed anchor cable bundle can significantly improve the stress state of the floor surrounding rock and achieve a good effect in weakening the stress of the floor surrounding rock. Therefore, the inhibitory effect of support scheme 3 on the displacement of the floor heave is considerable.

According to the research content of this article and engineering analogy experience, the surface displacement of the surrounding rock can directly reflect the supporting effect of the roadway and comprehensively reflect the stability of the surrounding rock. To comprehensively analyze the support effect of each support scheme, a detailed analysis of displacement should be performed so that the displacement of the floor heave change curve can be drawn, as shown in Figure 19. The numerical simulation results of the above-mentioned support schemes are sorted in Table 2.

Through the previous numerical simulation analysis, combined with Figure 19 and Table 2, the following conclusions are drawn:

(a) In the case of the unsupported state, because the roof of the roadway is fine-grained sandstone and the floor is mudstone, the displacement of the roof is smaller than that of the floor heave. The displacement of the roof and the floor heave are 78 mm and 494 mm, respectively. In addition, the total displacement of the roof and floor heave is 572 mm.

(b) In the case of the initial support scheme, the displacement of each part has been reduced. However, because the roadway support is not closed, the reduction of the displacement of the roof is limited. The displacement of the roof is reduced by 24%, and the displacement of the two roadway walls of the roadway is reduced by 42%. The supporting measures taken by the floor are insufficient, and the final displacement of the floor heave is 359 mm. Although the displacement of the floor heave has been reduced, it still cannot meet the needs of the working face.

(c) In support scheme 1, the displacement is significantly reduced compared to that of the unsupported condition. The displacement of the roof is reduced by 44%, and the

TABLE 2. Comparative Analysis of the Displacement of the Roadway in Each Scheme.

Support scheme	Displacement of the floor heave (mm)	Relative value	Displacement of the roof (mm)	Relative value	Displacement of the two roadway walls (mm)	Relative value
Unsupported	494	100%	78	100%	288	100%
Initial support scheme	359	72.7%	60	76.9%	167	58%
Support scheme 1	275	55.7%	46	59%	120	41.7%
Support scheme 2	185	37.4%	41	52.6%	102	35.4%
Support scheme 3	46	4.89%	46	4.89%	56	19.4%

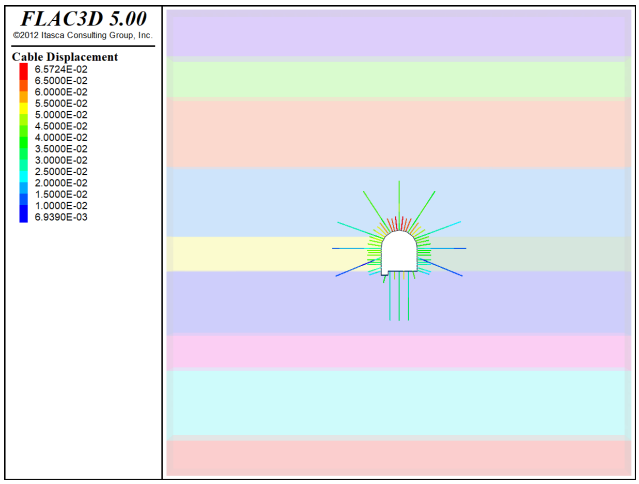

(a) Cloud diagram of the displacement

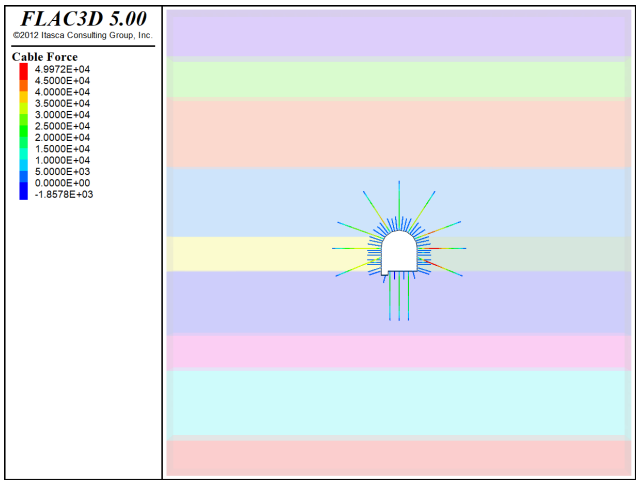

(b) Cloud diagram of the stress

FIGURE 17. Cloud diagram of the displacement and stress of the supporting structure.

displacement of the two roadway walls of the roadway is reduced by 58%. The final displacement of the floor heave is 275 mm.

(d) Through floor bolts and grouting support (support scheme 2), the grout fills the fractures of the surrounding rock around the roadway, which improves the overall strength of the surrounding rock, and the supporting effect is slightly improved compared to that of the scheme of applying only floor bolts. The final displacement of the floor heave is 185 mm.

(e) After adopting the combination support scheme of scheme 3 (floor bolts and grouting and prestressed anchor cable bundle), because of the tensile stress of the anchor cable, the limiting effect of the displacement on the floor is significantly enhanced. The final displacement of the floor heave is only 46 mm, which is 95% smaller than that of the unsupported state of the excavation. In addition, this support scheme produces a substantial decrease in the displacement of each part of the roadway.

Through comparative analysis, support scheme 3 is finally chosen for application to the engineering problem.

V. DISCUSSION (OPTIMIZATION ANALYSIS OF SUPPORTING PARAMETERS)

Although scheme 3 has been selected to support the roadway, from the perspectives of construction requirements, construction costs, and construction safety, the support scheme can also be optimized.

In terms of parameter optimization, it can be considered from two aspects: the specific construction process (such as drilling machine selection, installation steps of supporting components, etc.) and the difference in supporting parameters. Since the specific construction process cannot be realized in the numerical simulation, this article considers only the different support parameters. In the selected scheme 3, the supporting parameters of the roof and the two walls of the roadway have been measured by the relevant design department of the coal mine of Hebei province and are shown to meet the relevant design requirements. Therefore, this article optimizes only the floor support parameters that have been improved many times in the new scheme.

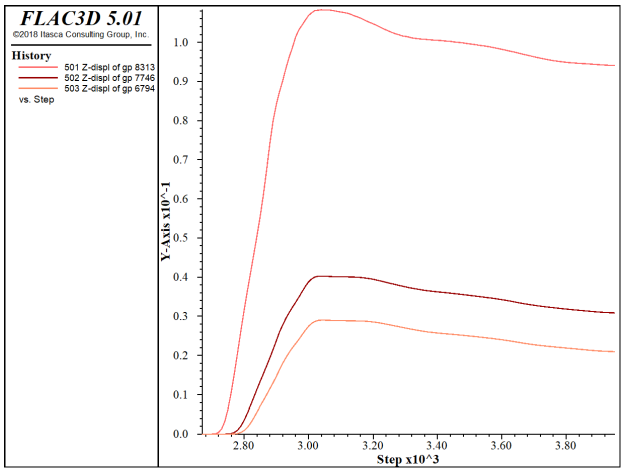

(a) New roadway support scheme 1

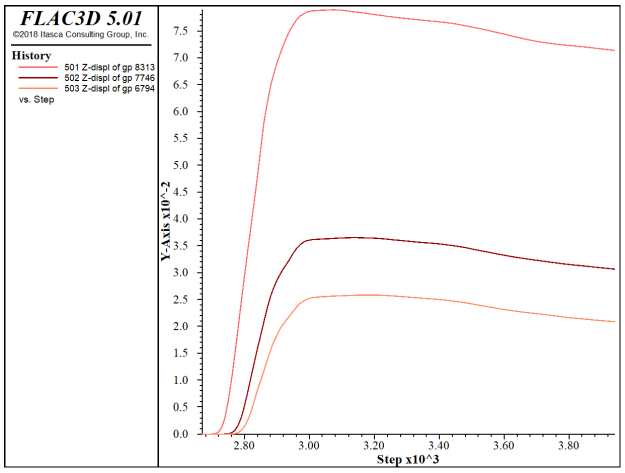

(b) New roadway support scheme 2

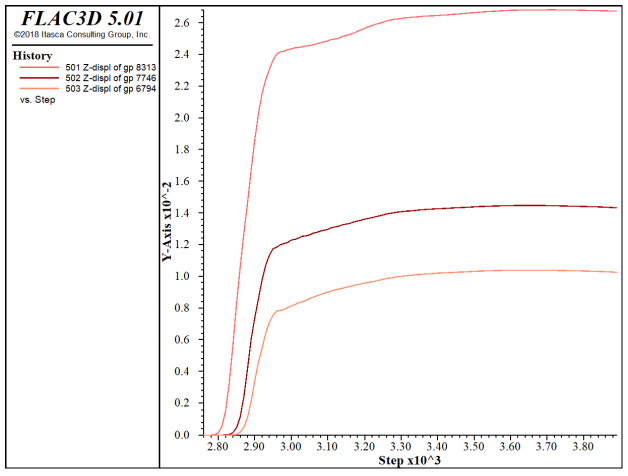

(c) New roadway support scheme 3

FIGURE 18. Vertical displacement monitoring curve of the floor of the three schemes.

Floor support parameters can be optimized, namely, the length of the floor bolts and grouting, the row spacing between the floor bolts and grouting, the length of floor anchor cable bundles, and the row spacing between the floor anchor cable bundles. However, in order to meet the

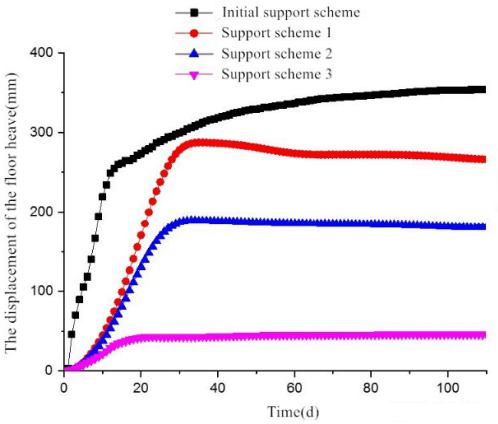

FIGURE 19. Vertical displacement monitoring curve of the floor of the three schemes.

requirements of the relevant design manual and achieve better support strength requirements in the scheme design, the length of the floor anchor cable bundles has been selected as a larger value. The row spacing between the floor bolts and grouting should not be too small (generally not less than 0.5 times the length of the bolts), nor too large (too close to the anchors or cables of the two walls of the roadway, which will lead a support structure that cannot be fully utilized). Therefore, this article optimizes only the length of the floor bolts and grouting and the row spacing between floor anchor cable bundles within a reasonable range. Through comprehensive consideration of construction requirements, construction costs, and construction safety, the optimized variables (1400 mm, 2000 mm) of the length of the floor bolts and grouting and the optimized variables of the row spacing between floor anchor cable bundles (1600 mm, 2100 mm) were determined. Four optimization methods are specifically designed:

Method 1: The length of the floor bolts and grouting is 1400 mm, and the row spacing of the floor anchor cable bundles is 1600 mm;

Method 2: The length of the floor bolts and grouting is 1400 mm, and the row spacing of the floor anchor cable bundles is 2100 mm;

Method 3: The length of the floor bolts and grouting is 2000 mm, and the row spacing of the floor anchor cable bundles is 1600 mm;

Method 4: The length of the floor bolts and grouting is 2000 mm, and the row spacing of the floor anchor cable bundles is 2100 mm.

The principal stress cloud diagram of the four optimization methods is shown in Figure 20 and Figure 21.

When the row spacing of the floor anchor cable bundles is 1600 mm, the maximum tensile stress on the floor of the roadway is approximately 0.5 MPa. Among these methods, method 3 produces the lowest stress value, followed by method 1. The reinforcement effect apparently is ideal when the row spacing of the floor anchor cable bundles is changed.

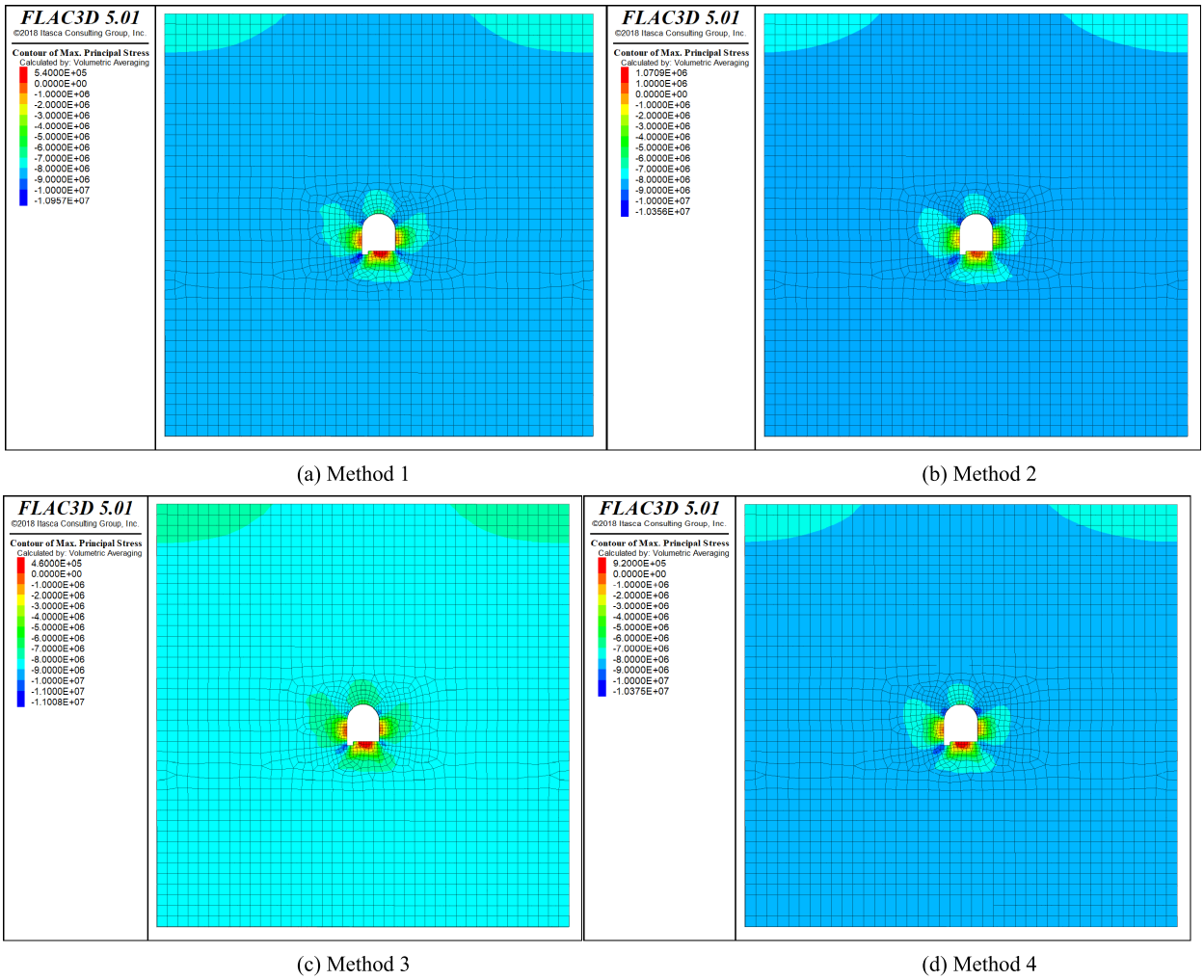

FIGURE 20. **Maximum principal stress cloud diagram of the four optimization methods.**

The contribution rate of the length of the floor bolts and grouting to changing the tensile stress of the floor is relatively low (Figure 20).

When the row spacing of the floor anchor cable bundles is 1600 mm, the maximum tensile stress on the floor of the roadway is approximately 0.5 MPa. Among these methods, method 3 produces the lowest stress value, followed by method 1. The reinforcement effect apparently is ideal when the row spacing of the floor anchor cable bundles is changed. The contribution rate of the length of the floor bolts and grouting to changing the tensile stress of the floor is relatively low (Figure 20).

Comparing the minimum principal stress cloud diagrams of the four optimization methods demonstrates that when three anchor cable bundles are used in the floor, i.e., the row spacing between the anchor cable bundles is 1600 mm, the stress concentration and range of the surrounding rock of the roadway are significantly reduced. Stress concentration only occurs at only the floor corner.

Within a certain depth below the floor, the stress concentration phenomenon is obviously improved. Comparing method 1 and method 3 shows that the effect of improving the stress concentration is not obvious when the floor bolts and grouting are changed. This result proves that the row spacing between the anchor cable bundles has a high contribution rate to the weakening effect of the stress concentration of the surrounding rock of the roadway floor. The floor anchor cable bundles share part of the ground stress that should be borne by the surrounding rock of the roadway, so that the surrounding rock stress on the surface of the roadway floor is transferred deeper. In addition, the total displacement cloud diagram of these four methods is illustrated in Figure 22.

The comparison diagram of the surrounding rock displacement on the roof and floor in the optimization methods is demonstrated in Figure 23.

Through the analysis of Figure 22 and Figure 23, the displacement of each part under various methods is summarized, as shown in Table 3, to have a more intuitive judgment on the optimal method.

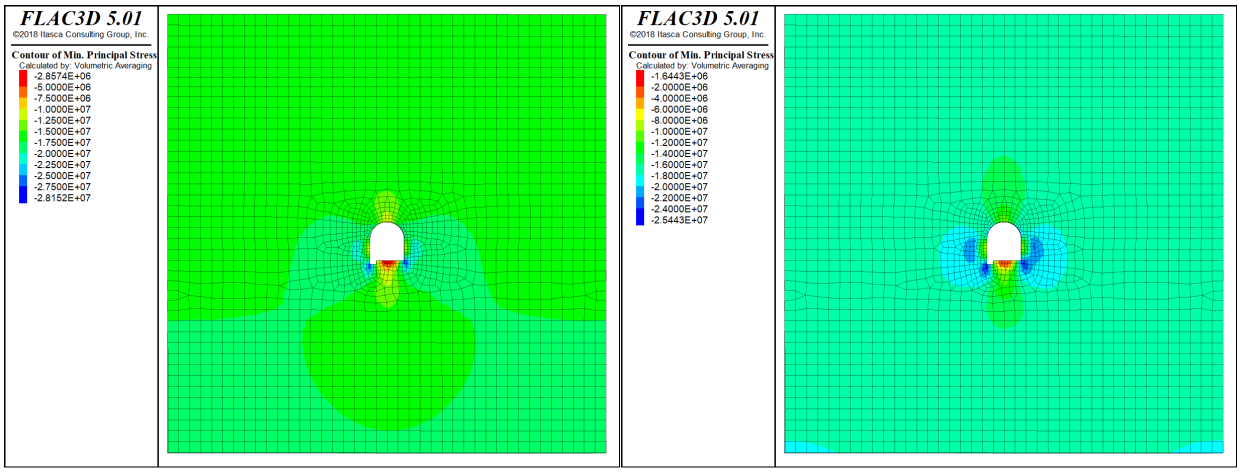

(a) Method 1 (b) Method 2

(c) Method 3 (d) Method 4

FIGURE 21. Minimum principal stress cloud diagram of the four optimization methods.

TABLE 3. The Displacement of Each Method in the Optimization Methods.

Method	Displacement of the floor heave	Displacement of the roof	Total displacement of the roof and the floor heave	Displacement of the left roadway wall	Displacement of the right roadway wall	Displacement of the two roadway walls
Method 1	46	25	71	30	26	56
Method 2	92	32	124	43	35	78
Method 3	42	25	67	29.3	25.3	54.6
Method 4	76	30.4	106.4	33.6	33.6	75.5

Based on the above data, the four optimization methods are compared and analyzed, and the following conclusions are drawn:

(a) In method 1 and method 2, the length of the floor bolts and grouting is 1400 mm, and only the row spacing of the floor anchor cable bundles is changed. The floor heave displacement of method 1 is significantly smaller than that of method 2. When the row spacing of the floor anchor cable bundles is 1600 mm, the supporting effect is stronger than when it is 2100 mm. The row spacing of the floor anchor

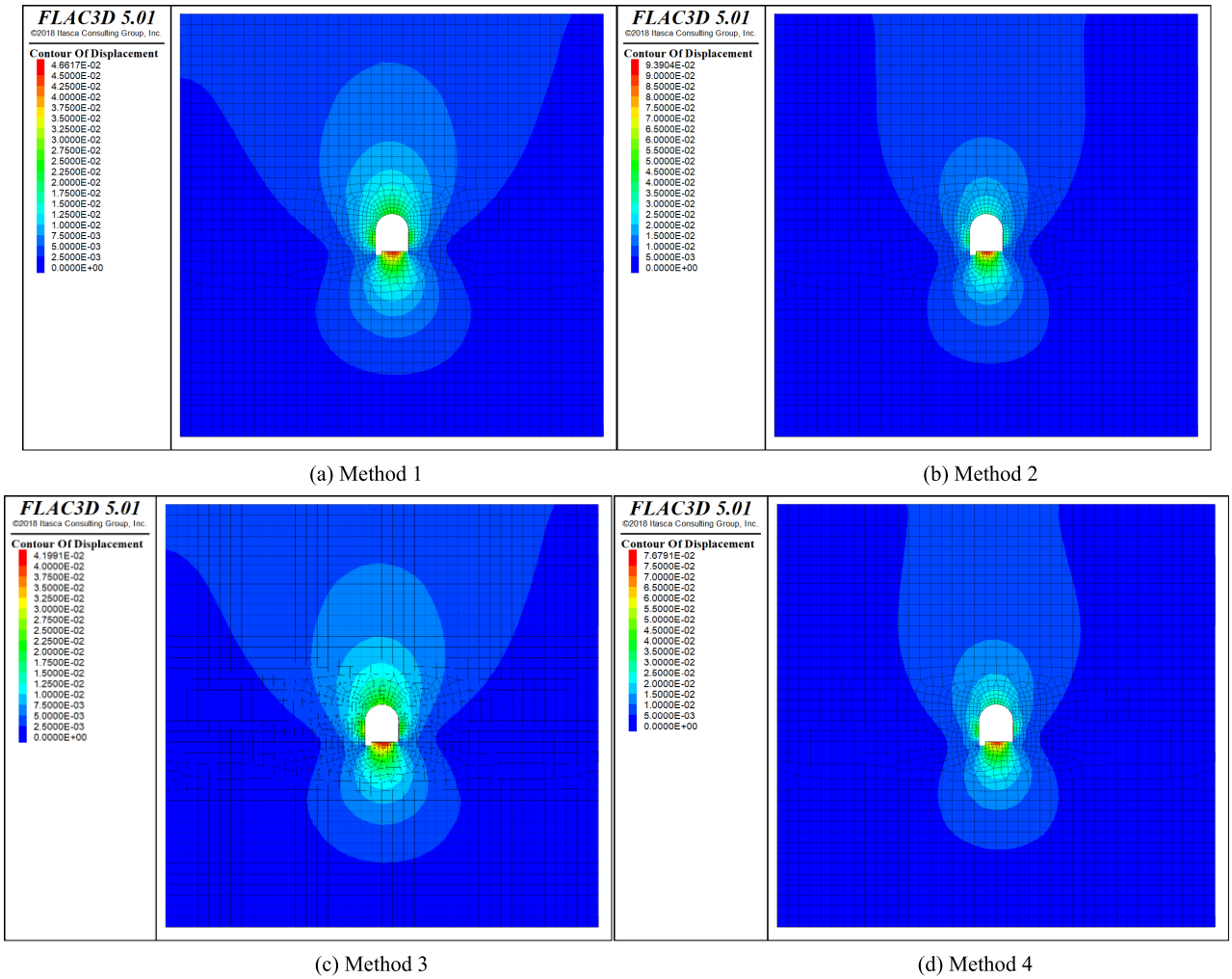

FIGURE 22. Total displacement cloud diagram of the four optimization methods.

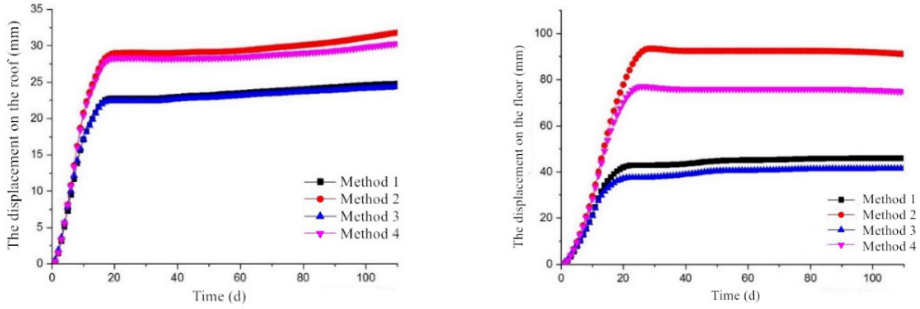

FIGURE 23. The comparison diagram of the surrounding rock displacement on the roof and floor in the optimization methods.

cable bundles apparently has a substantial effect on limiting the displacement of the floor.

(b) The row spacing of the floor anchor cable bundles is 1600 mm according to method 1 and method 3, and only the length of the floor bolts and grouting is changed. The displacement of each part of method 3 has a slight change compared with that of method 1, which shows that the change in the length of the floor bolts and grouting does not have a prominent impact on the support effect. Both a 1400-mm and 2000-mm length for the floor bolts and grouting can meet

the support needs of the roadway and working face. From economic considerations, the cost performance of method 1 is better than that of method 3.

(c) The comparison result of method 3 and method 4 is similar to that of method 1 and method 2, and the length of the floor bolts and grouting remains unchanged at 2000 mm. When only the length of the row spacing of the floor anchor cable bundles is changed, the displacement of the floor heave changes significantly, which further proves that the row spacing of the floor anchor cable bundles plays an important role in limiting the displacement of the floor.

Finally, optimization method 1 was adopted as the final support method, i.e., the length of the floor bolts and grouting is 1400 mm, and the length of the row spacing of the floor anchor cable bundles is 1600 mm, and these lengths are applied in the engineering problem.

Comparing the final selected scheme with the initial support scheme of the mine shows that the floor displacement decreased the most dramatically (by 87.2%), the roof displacement decreased by 58.3%, and the displacement of the two walls of the roadway decreased by 66.5%. It is not difficult to see that this scheme can restrain the displacement of surrounding rock more effectively than the initial support scheme and ensure the safety of roadway construction.

Moreover, in order to more easily quantify the multivariate uncertainty of the engineering system, we should also consider the confidence of the worst-case execution time (WCET) in the real-time system and understand the problems related to uncertainty and estimation/forecasting. Regarding this issue, related scholars have combined multiple algorithms such as evolutionary algorithms, and through many studies, established an adaptive proxy model and proposed a framework for determining the worst-case data [22]–[24]. The use of this predictive model can significantly reduce the verification time. Although this does not affect the research results of this article, for the follow-up research of the entire project, it can effectively improve the research efficiency and has important practical significance. The research in this article has been applied in actual engineering and has been well verified, but there are still many more in-depth studies to be done. Therefore, in order to quantify the multiple uncertainties of engineering systems more conveniently, more attention will be paid to the analysis of WCET in subsequent research.

VI. PROJECT ACTUAL APPLICATION EFFECT MONITORING

To verify the accuracy of the numerical simulation study, selected support scheme 3 is combined with optimization method 1 and applied to the actual project to conduct actual displacement monitoring.

A. LAYOUT OF THE MONITORING POINTS

After adopting the new roadway support scheme, a total of 3 displacement monitoring stations are arranged in the roadway, namely, station #1, station #2, and station #3, and the distance between stations is 5-6 m.

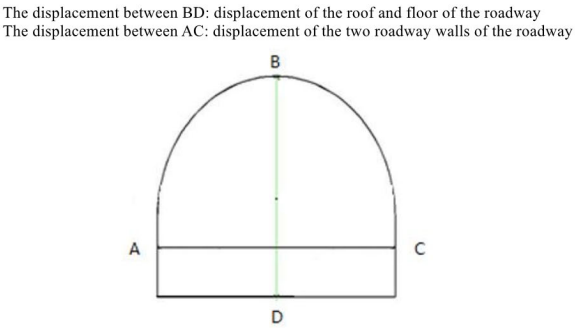

FIGURE 24. The arrangement of the displacement monitoring points.

The cross method is used to monitor the displacement change of the roadway surface. After the roadway support is reinforced, two groups of measuring points are set in each measuring station, namely, AC and BD (a total of 4 monitoring points were divided into two groups), as shown in Figure 24. Through the survey line BD, the displacement of the roof and floor of the roadway can be measured; through the survey line AC, the displacement of movement of the two roadway walls of the roadway can be measured. The monitoring period is two months.

B. ANALYSIS OF THE MONITORING RESULTS

To verify the accuracy of the numerical simulation study, selected support scheme 3 is combined with optimization method 1 and applied to the actual project to conduct actual displacement monitoring. The monitoring results are shown in Figure 25.

Figure 25 reveals that approximately 19 days after the excavation and support of the roadway, the displacement of the roof and floor changes greatly compared with that of the two roadway walls and the time required to stabilize the roof and floor is shorter.

1) At the location of station #1, the maximum displacement of the roof and floor was approximately 85 mm, and the displacement became stable on the 34th day; the displacement of the two roadway walls was approximately 76 mm, and the displacement became stable on the 28th day.

2) At the location of station #2, the maximum displacement of the roof and floor was approximately 80 mm, and the displacement became stable on the 38th day; the displacement of the two roadway walls was approximately 60 mm, and the displacement became stable on the 33th day.

3) At the location of station #3, the maximum displacement of the roof and floor was approximately 70 mm, and the displacement became stable on the 24th day; the displacement of the two roadway walls was approximately 72 mm, and the displacement became stable on the 41th day.

The monitoring results are compared with the previous numerical simulation analysis results as follows:

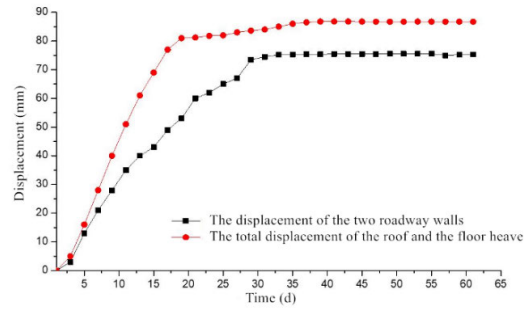

(a) Station 1#

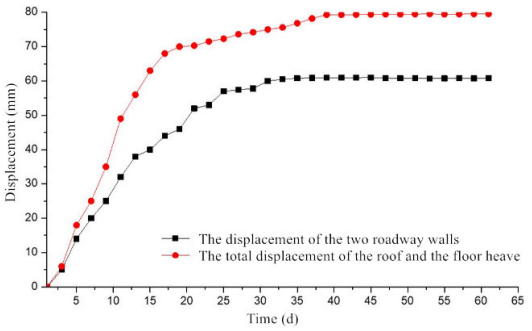

(b) Station 2#

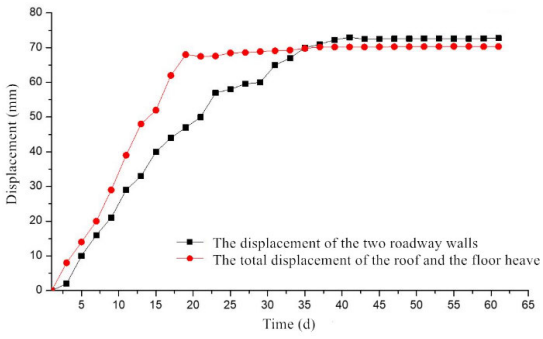

(c) Station 3#

FIGURE 25. Displacement convergence curve of each part of the roadway.

(a) Within 30 days after the excavation and support of the roadway, the displacement of the floor heave of the roadway gradually is shown to increase over time. When the rock mass around of the roadway reaches static equilibrium after excavation, the growth trend of the floor heave displacement gradually tends to be gentle. The change trends of the numerical simulation results and the actual monitoring results are basically identical.

(b) The displacement of the floor heave is approximately 40 mm according to the simulation and monitoring, and the displacement of the roof is approximately 20 mm. Among them, the floor displacement result obtained by numerical simulation is smaller than the actual monitoring value.

(c) The numerical simulation results and the actual mine pressure monitoring results are very similar. Because numerical simulation cannot restore the actual engineering geology, there must be a difference between the displacement of the surrounding rock calculated by numerical simulation and the project site monitoring value.

VII. CONCLUSION

Through PDM, combined with FLAC^{3D} software, a variety of support schemes were designed. FLAC^{3D} numerical simulation software was used to simulate and compare an unsupported roadway excavation, the initial support scheme of the roadway, and three new roadway support schemes. After selecting the optimal support scheme and optimizing the parameters, the scheme was applied to the actual project and achieved a good effect, and the following results were obtained:

1) Comparing and studying the stress cloud diagrams of different schemes, the presence of the anchor cable bundles of the floor has a small effect on the overall stress distribution in the entire model range but has a strong influence on the stress distribution around the roadway. When the roadway floor is in the unsupported state, the tensile stress on the floor is relatively large and the stress concentration is very severe. After the floor is reinforced, because of the presence of the anchor cable bundles, the stress value of the roadway floor is greatly reduced, the stress concentration is weakened, and the stress of the surrounding rock is gradually transferred deeper. When only floor bolts (support scheme 1) are used or only floor bolts and grouting (support scheme 2) are used, the tensile stress of the roadway floor is reduced, and the stress concentration phenomenon is also relieved to a certain extent; however, the supporting effect is obviously not as good as that of the floor bolts and grouting and the prestressed anchor cable bundle (support scheme 3).

2) The displacement cloud diagrams of the different schemes show that when the roadway floor is in an unsupported state, the floor heave displacement is larger than 494 mm and the displacement at a large depth range below the floor is at a relatively high level. Although the initial support scheme reduced the displacement to 359 mm, it could still not meet the requirements of safe production. After the three support schemes are used for reinforcement, the displacement of each part of the roadway is reduced. The effects of the single use of the floor bolts (support scheme 1) and the floor bolts and grouting (support scheme 2) are similar. When the floor bolts and grouting and prestressed anchor cable bundles (support scheme 3) are used for combined support, the supporting effect is the most ideal, and the floor heave displacement is significantly reduced compared with those of the other two schemes.

The fixed boundary restraint effect formed by the combined support (support scheme 3) reduces the floor heave displacement by 95% to 46 mm. The degree of change in the displacement directly reflects the restraint of the floor heave problem by the anchor cable bundles.

3) Support optimization analysis of the length of the floor bolts and grouting and the row spacing of the floor anchor cable bundles of the floor shows that the contribution rate of the row spacing of the floor anchor cable bundles to the suppression of the floor heave displacement is significantly greater than that of the floor bolts and grouting. From an economic perspective, it is finally determined that the length

of the floor bolts and grouting should be 1400 mm and the row spacing of the floor anchor cable bundles of the floor should be 1600 mm.

4) After the roadway was constructed according to support scheme 3, the roadway displacement was monitored for convergence and deformation. The monitoring data showed that the roadway floor had a certain displacement change in the early stage, the amount of change was small, and it tended to be stable in the later stage. The actual monitoring results have also proven the correctness of the numerical simulation research results. Comparison and analysis with the numerical simulation results show that the ideal effect was achieved for the support and reinforcement of the roadway floor and that the combined support (support scheme 3) of the floor bolts and grouting and the prestressed anchor cable bundles is feasible. This work has further fully proven the feasibility of the method and has provided an effective reference for engineering problems under similar geological conditions

REFERENCES

[1] Y. Bingqian, R. Fenhua, C. Meifeng, G. Qifeng, and Q. Chen, "Research progress of rock mechanics experiment and numerical simulation under THMC multi-field coupling," *J. Eng. Sci.*, vol. 1815, no. 3, pp. 1–12, 2019, doi: 10.13374/j.issn2095-9389.2019.07.29.005.

[2] G. Rui, Y. Jianfeng, C. Yushuo, and L. Wenji, "Research progress in numerical simulation of GTAW coupling model," *Heat Process. Technol.*, vol. 1807, no. 5, pp. 1–4, 2020, doi: 10.14158/j.cnki.1001-3814.20192511.

[3] L. Hongkun, L. Menglong, C. Wei, W. Mingjun, L. Kun, Y. Mingliang, and F. Jianren, "Research progress in numerical simulation of wind-induced response of transmission towers," *Steel Struct. (Chin. English)*, vol. 35, no. 4, pp. 1–10, 2020, doi: 10.13206/j.gjgS20051202.

[4] Q. Pengfei, "New progress in research on grouting technology for underground engineering," *Mod. Tunnel Technol.*, vol. 57, no. 2, pp. 55–60, 2020, doi: 10.13807/j.cnki.mtt.2020.02.008.

[5] D. Kong, M. Deng, and Y. Li, "Numerical simulation of seismic soil-pile interaction in liquefying ground," *IEEE Access*, vol. 8, pp. 195–204, 2020, doi: 10.1109/ACCESS.2019.2925664.

[6] Z. Guoping and Z. Mengxiao, "The development of marine numerical models and its application in marine biological diffusion simulation research," *Mar. Fisheries*, vol. 42, no. 2, pp. 245–256, 2020, doi: 10.13233/j.cnki.mar.fish.2020.02.012.

[7] X. Qingyan, Y. Cong, Y. Xuewei, and L. Baicheng, "Research progress in numerical simulation of directional solidification process of superalloy turbine blades," *Acta Metallurgica Sinica*, vol. 55, no. 9, pp. 1175–1184, 2019, doi: 10.11900/0412.1961.2019.00126.

[8] W. Tianyuan, X. C. Qingfeng, H. Lixin, M. Yuandong, and Y. Li, "Research progress in numerical simulation of microbial flooding," *J. Central South Univ. (Natural Sci. Ed.)*, vol. 50, no. 6, pp. 1474–1484, 2019, doi: 10.11817/j.issn.1672-7207.2019.06.027.

[9] L. Pei, X. Gong, and S. Xuan, "Recent progress on the simulation technology of magnetic fluid," *Chin. Sci. Bull.*, vol. 64, no. 15, pp. 1567–1582, May 2019, doi: 10.1360/N972018-01068.

[10] H. Bo, "Advances in numerical simulation technology of chemical flooding in high-temperature and high-salt reservoirs," *Oil Gas Geol.*, vol. 39, no. 6, pp. 1305–1310, 2018, doi: 10.11743/ogg20180619.

[11] L. Zhang, Z. Sun, C. Zhang, F. Dong, and P. Wei, "Numerical investigation of the dynamic responses of long-span bridges with consideration of the random traffic flow based on the intelligent ACO-BPNN model," *IEEE Access*, vol. 6, pp. 28520–28529, 2018, doi: 10.1109/ACCESS.2018.2840333.

[12] P. Cao, Q. Shuai, and J. Tang, "Leveraging Gaussian process regression and many-objective optimization through voting scores for fault identification," *IEEE Access*, vol. 7, pp. 94481–94496, 2019, doi: 10.1109/ACCESS.2019.2924713.

[13] R. Barcena, T. Acosta, A. Etxebarria, and I. Kortabarria, "Wind turbine structural load reduction by linear single model predictive control," *IEEE Access*, vol. 8, pp. 98395–98409, 2020, doi: 10.1109/ACCESS.2020.2996381.

[14] G. Li, Y. Hu, Q.-B. Li, T. Yin, J.-X. Miao, and M. Yao, "Inversion method of *in-situ* stress and rock damage characteristics in dam site using neural network and numerical simulation—A case study," *IEEE Access*, vol. 8, pp. 46701–46712, 2020, doi: 10.1109/ACCESS.2020.2979024.

[15] E. Wu, R. Huang, L. Wu, X. Shen, and Z. Li, "Numerical study on the influence of altitude on roof temperature in mine fires," *IEEE Access*, vol. 8, pp. 102855–102866, 2020, doi: 10.1109/ACCESS.2020.2997919.

[16] J. Chang, G. Xue, and R. Malekian, "A comparison of surface-to-coal mine roadway TEM and surface TEM responses to water-enriched bodies," *IEEE Access*, vol. 7, pp. 167320–167328, 2019, doi: 10.1109/ACCESS.2019.2953844.

[17] W. Tao, H. Xuan, Z. Xianyu, and Z. Yongsheng, *FLAC 3D Numerical Simulation Method and Engineering Application*, 1st ed. Beijing, China: China Building Industry Press, 2015, pp. 1–9.

[18] Y. Du, G. Feng, Y. Zhang, X. Zhang, Y. Zhai, and J. Bai, "Pressure reduction mechanism and effect of working face passing through abandoned roadway by roof presplit," *Energy Sci. Eng.*, no. 1, pp. 1–12, Jul. 2020, doi: 10.1002/ese3.760.

[19] C. Zhu, Y. Yuan, Z. Chen, Z. Liu, and C. Yuan, "Study of the stability control of the rock surrounding double-key strata recovery roadways in shallow seams," *Adv. Civil Eng.*, vol. 2019, pp. 1–21, Aug. 2019, doi: 10.1155/2019/9801637.

[20] C. Yuan, L. Fan, J.-F. Cui, and W.-J. Wang, "Numerical simulation of the supporting effect of anchor rods on layered and nonlayered roof rocks," *Adv. Civil Eng.*, vol. 2020, pp. 1–14, Jan. 2020, doi: 10.1155/2020/4841658.

[21] W. HaiTao, C. Tong, W. YaJun, L. Tao, and Q. N. Hua, "Research of mechanical characteristics and roadway support in two-soft and one-hard coal seam," in *Proc. Int. Conf. Green Buildings Environ. Manage.*, vol. 186, 2018, doi: 10.1088/1755-1315/186/5/012032.

[22] I. Bate, D. Griffin, and B. Lesage, "Establishing confidence and understanding uncertainty in real-time systems," in *Proc. 28th Int. Conf. Real-Time Netw. Syst.*, Jun. 2020, pp. 67–77, doi: 10.1145/3394810.3394816.

[23] S. A. B. Shah, M. Rashid, and M. Arif, "Estimating WCET using prediction models to compute fitness function of a genetic algorithm," *Real-Time Syst.*, vol. 56, no. 1, pp. 28–63, Jan. 2020, doi: 10.1007/s11241-020-09343-2.

[24] M. Rashid, S. A. B. Shah, M. Arif, and M. Kashif, "Determination of worst-case data using an adaptive surrogate model for real-time system," *J. Circuits, Syst. Comput.*, vol. 29, no. 1, Jan. 2020, Art. no. 2050005, doi: 10.1142/S021812662050005X.

YUE WU is currently pursuing the Ph.D. degree in geotechnical engineering with the Shandong University of Science and Technology, China. His research interests include the deep rock fracture failure, grouting, support, and the inoculation mechanism of discontinuous fractured rock.

WEIGUO QIAO received the Ph.D. degree. He is also a Professor and a Doctoral Supervisor of Geotechnical Engineering, a Famous Teacher with the Shandong University of Science and Technology, and the Director of the Academic Affairs Office. He was a recipient of the Excellent Talents in China's Coal Industry Technology Innovation, the Excellent Talents in the New Century by the Ministry of Education, and the Young and Middle-Aged Experts with Outstanding Contributions in Shandong Province. He concurrently serves as a member of the Rock Mechanics and Support Professional Committee of China Coal Society, the Vice Chairman of the Shandong Rock Mechanics and Engineering Society, the Executive Director of the Underground Engineering Branch of China Rock Mechanics and Engineering Society, a Mine Construction Expert of the China Coal Industry Technical Committee, and the China Coal Industry Association's Expert.

SHUAI ZHANG is currently pursuing the Ph.D. degree in geotechnical engineering with the Shandong University of Science and Technology, China. His research interests include the grouting support for micro-fractured rock masses and the seepage law of cement slurry.

ZONGHAO ZHANG received the master's degree from the Shandong University of Science and Technology, China. His research interest includes the deep underground engineering support.

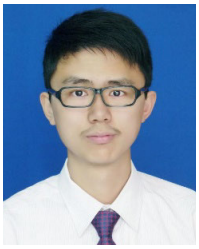

YANZHI LI is currently pursuing the Ph.D. degree in geotechnical engineering with the Shandong University of Science and Technology, China. His research interests include the deep well sandstone microscopic pore seepage characteristics and cavity expansion grouting water plugging mechanism.

ZHENWANG FAN is currently pursuing the master's degree in geotechnical engineering with the Shandong University of Science and Technology, China. His research interest includes the sandstone micro-pore model research.

LEI ZHANG is currently pursuing the master's degree in geotechnical engineering with the Shandong University of Science and Technology, China. His research interests include the rock micropore seepage characteristics and grouting water plugging.